



Cooperative Research Centre for  
Landscape Environments  
and Mineral Exploration



**action**  
Salinity & Water  
AUSTRALIA



**Government  
of South Australia**



**OPEN FILE  
REPORT  
SERIES**



**Australian Government  
Geoscience Australia**

# **3D REGOLITH ARCHITECTURE OF THE JAMESTOWN AREA - IMPLICATIONS FOR SALINITY**



*J. Wilford*

**CRC LEME OPEN FILE REPORT 178**

**September 2004**

CRCLEME

CRC LEME is an unincorporated joint venture between CSIRO-Exploration & Mining, and Land and Water, The Australian National University, Curtin University of Technology, University of Adelaide, Geoscience Australia, Primary Industries and Resources SA, NSW Department of Mineral Resources and Minerals Council of Australia, established and supported under the Australian Government's Cooperative Research Centres Program.





Australian Government  
Geoscience Australia



# 3D REGOLITH ARCHITECTURE OF THE JAMESTOWN AREA - IMPLICATIONS FOR SALINITY

*J. Wilford*

**CRC LEME OPEN FILE REPORT 178**

September 2004

*Report prepared for the South Australia Salinity Mapping and  
Management Support Project.*

*This project is jointly funded by the South Australian and Commonwealth  
Governments under the National Action Plan for Salinity and Water Quality.*

© CRC LEME 2004

---

CRC LEME is an unincorporated joint venture between CSIRO-Exploration & Mining, and Land and Water, The Australian National University, Curtin University of Technology, University of Adelaide, Geoscience Australia, Primary Industries and Resources SA, NSW Department of Mineral Resources and Minerals Council of Australia.

*Headquarters:* CRC LEME c/o CSIRO Exploration and Mining, PO Box 1130, Bentley WA 6102, Australia

© CRCLEME

**Copies of this Publication can be obtained from :**

The publications Officer, CRCLEME, c/- CSIRO Exploration and Mining, PO Box 1130, Bentley WA 6120, Australia. Information on other publications in this series may be obtained from the above, or from <http://crcleme.org.au>

**Cataloguing-in-Publication:**

Name: Wilford, J., Title: 3D Regolith architecture of the Jamestown area – implications for salinity

ISBN 1 921039 16 7

1. Jamestown, South Australia 2. Regolith architecture 3. Salinity

I. Name II. Title

CRCLEME Open File Report 178

ISSN 1329-4768

**Address and Affiliation of Authors**

**John Wilford**

Cooperative Research Centre for Landscape  
Environments and Mineral Exploration  
Geoscience Australia  
GPO Box 378,  
Canberra, ACT 2601  
Australia

© Cooperative Research Centre for Landscapes,  
Environment and Mineral Exploration, 2004

## TABLE OF CONTENTS

<b>1. INTRODUCTION .....</b>	<b>1</b>
1.1 Background and rationale for the study .....	1
1.2 Objectives.....	1
1.2.1 Specific Objectives.....	1
<b>2. APPROACH .....</b>	<b>2</b>
<b>3. STUDY AREA AND REGIONAL SETTING .....</b>	<b>3</b>
3.1 Location and geophysical survey areas.....	3
3.2 Climate, vegetation and land use.....	4
3.3 Geology, physiography and soils .....	4
<b>4. HYDROGEOLOGY.....</b>	<b>12</b>
4.1 Origin of salt and dryland salinity.....	12
<b>5. STUDY METHODS – data acquisition and processing.....</b>	<b>13</b>
5.1 Gamma-ray spectrometry and magnetics .....	13
5.1.1 Gamma-ray spectrometry .....	13
5.1.2 Magnetics .....	15
5.2 Digital elevation model .....	15
5.3 Airborne EM .....	15
5.4 Drill hole information and surface soil sampling .....	18
5.5 Ground geophysics.....	22
5.5.1 EM31 .....	22
<b>6. RESULTS.....</b>	<b>23</b>
6.1 Interpretation of airborne spectrometry.....	23
6.1.1 Gamma-ray response of bedrock and regolith.....	23
6.2 Terrain analysis .....	28
6.2.1 Delineation of major morphological and hydrological characteristics.....	28
6.3 Interpretation of airborne magnetics .....	33
6.2.1 Delineation of magnetic drainage channels.....	33
6.4 Interpretation of airborne EM .....	36
6.5 Sedimentary Facies .....	38
6.6 3D architecture model of the evolution of the valley fill sequence and implications for salinity.....	43
<b>7. CONCLUSIONS.....</b>	<b>49</b>
<b>8. ACKNOWLEDGEMENTS.....</b>	<b>50</b>
<b>9. REFERENCES.....</b>	<b>51</b>

## LIST OF FIGURES

**Figure 1.** Location of study area and position of geophysical surveys

**Figure 2.** Geological map.

**Figure 3.** Hillshaded digital elevation model with roads, towns and surface drainage. Spot height elevations show relative changes in relief.

**Figure 4.** Hillshaded DEM with surface drainage in purple. The yellow line delineates slopes above and below 1.5 degrees and in most places separates erosional landforms (> 1.5 degrees) from depositional landforms (< 1.5 degrees).

**Figure 5.** 3D perspective view of the 1945 soil map (Stephens, et al. 1945) draped over the digital elevation model.

**Figure 6.** Major Soil Land Systems (PIRSA, 2001). See text for descriptions.

**Figure 7.** Areas of dryland salinity and TDS concentrations from bores.

**Figure 8.** Pseudo-coloured and three band false colour composite image of K, eTh and eU.

**Figure 9.** CDI slices with hillshaded DEM and drainage attributes added. All image scale from 0 – 200 mS/m.

**Figure 10.** Location of interpreted drill holes

**Figure 11.** Interpreted drill hole sections and drill log key.

**Figure 12.** Location of soil samples and an unsupervised classification of the K, eTh and slope was used to stratify surface soil sampling. This allowed samples to be collected that reflected a range of landform and gamma-ray responses.

**Figure 13.** 3D perspective drape of 3-band gamma-ray spectrometry image over the digital elevation model. The line delineates slopes above (erosional landscapes) and below 1.5 degrees (depositional landscapes).

**Figure 14.** Relationship between surface soil silt content and airborne K concentration. Samples plotted for deposition landscapes only.  $R^2 = 0.6$ .

**Figure 15.** Modelled surface soil silt content based on the correlation between airborne K and silt. The Belalie and to a less extent Bundaleer depositional plains have significantly more silt than the Caltowie catchment.

**Figure 16.** 3D perspective image of the 3-band gamma-ray draped over the digital elevation model. Colluvial fan developed along the east edge of the Bundaleer Range are highlighted. Rocks contributing sediment to these fans are high in each of the three radioelements.

**Figure 17.** Slope map derived from the DEM.

**Figure 18. A** - Location of topographic profiles across the Belalie, Bundaleer and Caltowie valleys. **B** - Topographic profiles across the Belalie, Bundaleer and Caltowie valleys. Refer to figure 15 A for locations.

**Figure 19.** Drainages derived from the digital elevation model. Drainage segments are coloured according to their gradients. Low stream gradients in yellow – higher gradients in pink to red.

**Figure 20.** Magnetic image showing magnetic channel drainage lines and present day drainage in blue.

**Figure 21.** Perspective magnetic image highlighting magnetic river channels draped over the DEM.

**Figure 22. A** – Original drainage network (purple) and flow direction (yellow) as delineated from the magnetic drainage lines. **B** – Superimposed drainage developed as a result of infilling the upper part of

the Belalie valley. Surface drainage now flows into the Bundaleer valley, although sub-surface groundwater is likely to still flow down the Belalie Valley.

**Figure 23.** Magnetic drainage lines superimposed over the 10-15 m CDI slice.

**Figure 24.** 0-5m CDI with areas of known dryland salinity (white polygons).

**Figure 25.** A – Belalie valley, B – colluvial fan down slope from the Bundaleer Range, C – carbonate root casts, D – poorly sorted debris flow deposits, E – alluvial sediments with platy carbonate layers and F – channel gravels (traction deposit)

**Figure 26.** A – Carbonate precipitating along joints and fractures within saprolite, B – eroded terraced alluvium eastern side of the Belalie valley, C – roots/worm burrows replaced by carbonate, D – highly weathered structured saprolite with a veneer of silty soil, E – maghemite gravels and F – groundwater carbonate precipitating along the saprolite – sediment contact.

**Figure 27.** A – lithosols on bedrock, typically of the upland areas, B – low angle colluvial fan, C – incised sheet flood fan sediments east of Jamestown, D – highly weathered and mottled saprolite NNW of Caltowie, E – erosional scars on shallow soils on saprolite and F – valley fill sediments in the lower part of the Belalie valley

**Figure 28.** A – Rises in the upper part of the Caltowie catchment, B – river channel gravels consisting of ferruginous lithic fragments, quartz and minor maghemitic gravels, C – lithosols on low hills, D – dissolution depression caused by the removal of carbonate in the bedrock. These solution features collect water and are usually highly saline, E – incised alluvial sediments in the upper part of the Belalie valley and F – skeletal soils on low hills.

**Figure 29.** Position of selected drill logs and 3D perspective gamma-ray image.

**Figure 30.** Major groundwater basins and agricultural districts.

**Figure 31.** Base of the AEM conductor (50 m/Sm threshold used) coloured according to the thickness. In most cases this represents the sediment isopach in each of the three main valley systems. Indicative thickness of sediments shown. Magnetic channels in yellow. Conductive basement rocks are difficult to separate from the valley sediments, although because there are generally much deeper features they can be easily identified in the imagery.

**Figure 32.** BRS holes JT8 and JT5 showing geology, 1:5 EC, moisture, gamma, EM39 and magnetic susceptibility. See figure 29 for the location of these holes in relation to the whole study area.

**Figure 33.** Regolith-landscape evolution model for the upper part of the Belalie and Bundaleer River catchments. Based on drilling, terrain analysis and geophysical interpretation.

## ABSTRACT

The combined analysis of a digital elevation model, gamma-ray spectrometry, magnetics, airborne electromagnetics (AEM) and drill holes has provided new insights into the regolith-landform evolution of the Jamestown region, located in the Mid North of South Australia. In particular, the 3D architecture (geometry and composition) of the valley fill deposits is better understood. Three dimensional models generated from the integration of these datasets show the distribution of regolith materials, salt stores and possible preferential flow paths for groundwater in the region.

The Jamestown region is characterised by a range of landforms from low relief colluvial and alluvial fans, floodplains and pediments through to rises, low hills and hills. Depositional materials occur in three main valleys: the Belalie, Bundaleer and Caltowie. Coalescing colluvial and alluvial fans of Quaternary age have filled these valleys to depths of up to 40 metres. The thickest sediments consisting of silt, clay, fine sand and minor gravels occur in the Belalie and Bundaleer valleys. The Caltowie valley has a thinner sediment cover which appears to have a lower electrical conductivity when compared with the other two catchments. Low angle pediments characterise the upper parts of the Caltowie catchment.

Airborne gamma-ray spectrometry was effective in separating a variety of bedrock types and regolith materials based on their radioelement characteristics. A relationship between the surface texture of soils on depositional plains and airborne K concentrations was used to predict the surface silt content in each of the main valleys. The Caltowie valley has less silt and a higher percentage of medium to fine sand than the other two catchments. Whether these sandier soils are representative of materials at depth is not known. Most of the sediments in these valley systems are dominated by poorly sorted debris or mudflow deposits that consist mostly of silt and clay with minor gravels. Available drilling suggests that scattered throughout the valley fill, but more common in the basal part of the alluvial sequence, are traction or bed load deposits associated with river channels. Many of these buried channel sediments contain maghemite that are clearly delineated in high frequency component of the airborne magnetic imagery. Magnetic channels show rill, dendritic and braided patterns. In areas of thicker sediment cover, inter-woven and possibly stacked, buried palaeo-channel networks are observed in the magnetic imagery. These buried palaeo-channels define a palaeo-darainge system that is not reflected in the contemporary drainage, which is widely spaced and discontinuous. As a result of the Belalie valley being partly filled with sediment there is evidence of superimposed drainage diverting palaeo-drainage lines east of Jamestown.

With the exception of some local discrete conductive basement rocks, the valley fill sediments and some areas of highly weathered saprolite appear, in the airborne EM, as the most conductive materials in the landscape. An isosurface (3D surface of equal value) of the high, near-surface conductivity in most cases delineates the geometry of the valley prior to sedimentation and infilling. Both the fine grained sediments of the valley fill and highly weathered bedrock are likely to contain the highest salt stores as implied by an interpretation of the AEM data.

Overlaying the salt stores (defined using the AEM) on the magnetic channels highlights possible groundwater flow directions. The surface expression of dryland salinity within the valleys occurs where salt stores and associated regolith materials thin and where basement barriers or valley constrictions impede groundwater flow. Valley constrictions and associated dry land salinity occur in the Bundaleer and Caltowie valleys but not the Belalie valley, despite the fact that the Belalie valley has the highest salt store. This might be explained by the fact that the Belalie system has a relatively thick transported cover with numerous buried, and more transmissive and inter-connected channel networks. It is proposed that this more effective sub-surface drainage may prevent the build up of shallow water tables and salts in the upper soil layer.

## **1. INTRODUCTION**

### **1.1 Background and rationale for the study**

Dryland salinity and salinisation of rivers is a major problem throughout agricultural regions in Australia. To help resolve environmental issues arising from these concerns there is a need to better understand where the salt is stored, and to determine how these stores interact with ground and surface water. These problems affect the region around Jamestown, located in South Australia's Northern Agricultural District, which constitutes some of South Australia's most productive agricultural land. The area currently has approximately 10% of its land affected by dryland salinity (Henschke, 1994), with a continuing threat from rising saline groundwater. The area of affected land is of concern to the local community in terms of lost productivity, salt-induced soil erosion and urban infrastructure damage caused by rising, saline groundwaters (eg. townships of Jamestown and Caltowie). To better manage this threat, an improved knowledge of groundwater, soils and salinity distribution, along with an understanding of recharge processes is recognised as being important. This information is needed at regional scales for select valleys.

Groundwater models need to be developed to examine various management options for these systems, including the lowering of water tables in the valleys by pumping, deep drainage and/or the re-introduction of deep-rooted perennial crops. To help better constrain these models there is a need to define the general shape of the valley fills, identify the salt stores and the likely movement of saline groundwater through the landscape. There is also a need to understand the variability of these materials in the landscape.

In this context, the principal aim of this study was to better understand the relationships between geology, landform, regolith materials and associated weathering and geomorphic processes that are likely to constrain the distribution of salt and the hydrogeology of the Jamestown landscape. The basic premise behind this work was the notion that the regolith has an important bearing on groundwater recharge, groundwater movement and storage, and the storage of soluble salts. Many areas of dryland salinity occur across a diverse regolith cover that may be up to several hundred metres thick. The depth of weathering, permeability, and the physical characteristics of the regolith aquifer system needs to be considered when developing an improved hydrogeological model for the region.

### **1.2 Objectives**

The primary objective of this study was to map the nature and distribution of regolith materials in three dimensions (3D) across the Jamestown region. Particular emphasis has been placed on the origin and characteristics of valley fill deposits, as these materials are believed to hold most of the stored salt in the landscape. This information is aimed at constraining hydrogeological models that will be developed for the area by Bureau of Rural Sciences (BRS) and State Project Partners.

#### ***1.2.1 Specific Objectives***

1. Define a regolith-landscape framework that describes the nature, origin and distribution of regolith materials in three dimensions. Particular attention is given to the geometry and characteristics of these landforms and materials.
2. Map the distribution of regolith materials using gamma-ray spectrometry, magnetic and electromagnetic data.
3. Determine the relationships between regolith materials and salinity in the landscape.

## 2. APPROACH

Mapping regolith materials and understanding palaeo/present day geomorphic processes is generally seen as the first step in developing conceptual models to account for how these materials have evolved through time and how they are distributed in the landscape. Once the inter-relationships between regolith materials, landscape and processes are understood, more effective and predictive models of regolith type, structure and thickness can be developed. This information can then be directed towards developing more robust hydrogeological models by providing constraints on the sub-surface controls of groundwater movement and the storage and mobilisation of salts in areas of regolith cover.

In this study, the nature and distribution of regolith materials and landforms are described through the combined interpretation of airborne gamma-ray, magnetic and electromagnetic (AEM) data, along with digital elevation modelling, existing soil and geological datasets. Field observations, soil sampling and drilling provided ground validation for these datasets. Specifically, the datasets used here provide the following information:

**Gamma-ray spectrometry** - description of soil and regolith materials types. Gamma-ray patterns inform on geomorphic and weathering processes. Existing soil and geological maps assist in the interpretation of the radioelement responses.

**Magnetics** - delineation of geological units, geological structures and palaeochannels. These are used in conjunction with present-day drainage to form a framework that describes the drainage evolution of the area.

**Airborne EM** - provides conductivity-depth information that can be used to map the distribution and thickness of conductive and non conductive regolith materials. If conductivity contrasts exist between saprolite and the overlying transported materials a sedimentary isopach map will be generated. This will be used by BRS to model the groundwater aquifer using FLOWTUBE ([http://agspsrv34.agric.wa.gov.au/environment/tools/flowtube/what\\_is\\_flowtube.htm](http://agspsrv34.agric.wa.gov.au/environment/tools/flowtube/what_is_flowtube.htm)). In areas where conductive lithological units are present (e.g. carbonaceous shales), these may be mapped using the AEM data.

**DEM** - terrain analysis provides information on the type and distribution of landforms. Perspective drapes and cross-sections are used to understand landscape control on the distribution of regolith materials and on how particular landforms may be linked to geology and structure. Surface hydrological characteristics are delineated including catchment boundaries, river gradients and likely groundwater discharge sites (e.g. topographic wetness index).

**Drilling** - provides control on the interpretation of all geophysical datasets, particularly the AEM. It also informs on the nature of transported and *in-situ* regolith. Drill cuttings and core are also analysed for geochemistry, mineralogy, electrical conductivity (EC 1:5) and texture.

These datasets are then interpreted and combined to generate a 3D regolith-landform model of the Jamestown area. Schematic cross-sections developed from selected traverses provide insights into relationships between regolith materials, topography and landscape processes.

### 3. STUDY AREA AND REGIONAL SETTING

#### 3.1 Location and geophysical survey areas.

The study area is located within the 1:250 000 Burra map sheet in the mid-north of South Australia and includes the townships of Jamestown and Caltowie (Figure 1). The airborne gamma-ray spectrometry, magnetics and digital elevation model were acquired over an area of approximately 28km E-W and 35Km N-S. The airborne EM survey was restricted to the top northern half of the study area (Figure 1).

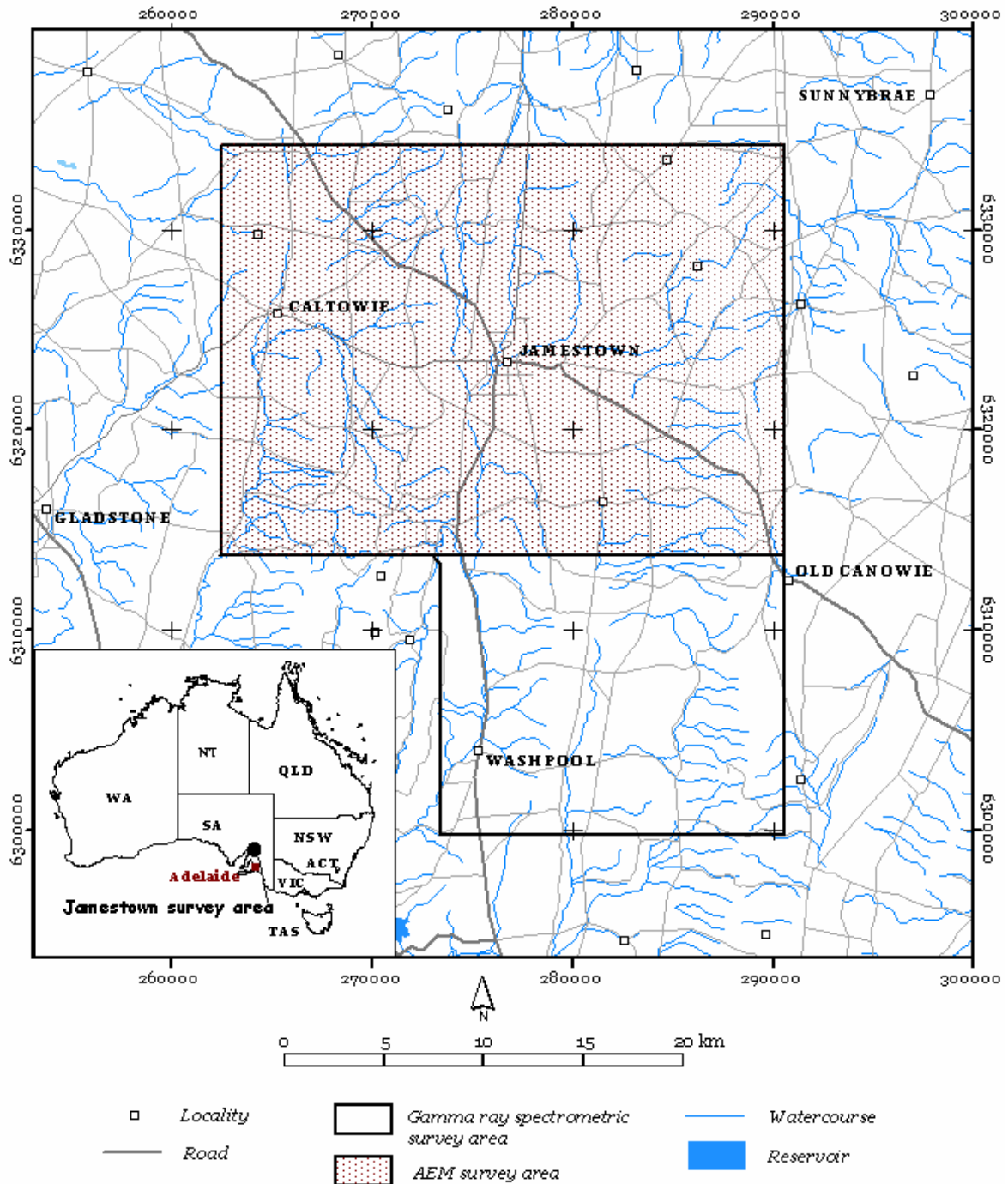


Figure 1. Location of study area and position of geophysical surveys.

### 3.2 Climate, vegetation and land use

The area has cool wet winters and typically hot dry summers. Jamestown has an average annual rainfall of about 460mm. Evaporation rates exceed rainfall throughout the year (Bureau of Meteorology, unpublished data - cited from Henschke, 1994). The native vegetation prior to farming in 1870 (Cooper, 1978) probably consisted of open savannah. Low-lying areas along valley floors and adjacent low gradient alluvial and colluvial slopes were thought to be dominated by grasses, including *Darthonia semi-annularis* (wallaby grass), *Lomandra dura* (iron grass) and *Themeda triandra* (Stephens, et al., 1945). Elevated sites with better drainage probably supported a woody cover with a grassy understorey. Woody species included; *Casuarina stricta* (sheoak) *Acacia spp* (wattle) and *Eucalyptus odorata* of mallee habit (Henschke, et al., 1994 and Stephens, et al., 1945). Present day land use includes cropping (wheat, lucerne, field peas) and sheep grazing. Soft pine plantations provide timber for timber milling operations.

### 3.3 Geology, physiography and soils

Basement rocks in the area consist of Proterozoic sediments of the Umberatana and Burra Groups. The lithologies include siltstones, dolomites, sandstones, quartzites, limestones, tillites, feldspathic sandstones, pyrite shales, calcareous siltstones and sandstones (Figure 2). Structural deformation and associated contact and regional metamorphism has folded and altered these rocks. Phyllite and hornfels textures are common. The overall structural trend is North-South with anticlinal and synclinal folds clearly delineated on the hill-shaded digital elevation model (Figure 3). Locally acid intrusive lithologies (north-east corner of the study area) outcrop but predominantly the basement rocks are sedimentary.

The metamorphosed Proterozoic sediments have a strong topographic expression. Quartzite (e.g. Gilbert Range Quartzite) and siliceous tillite beds are more resistant to weathering and form prominent steep bedrock ridges. Less resistant siltstones and carbonates have been eroded to form a series of North-South elongated valleys. These include the Belalie, Bundaleer and Caltowie valleys (Figure 3). Quaternary alluvium and colluvial fans have in-filled these valleys to depths of up to 40 metres. The highest relief is associated with the Brown Range along the eastern side of the Belalie valley and the Bundaleer Range over the central part of the study area. Low-angle pediments characterise the upper parts of the Caltowie catchment. Slopes within the study area vary between 0 to 30 degrees. Based on field traverses, slopes less than 1.5 degrees generally separate low-angle colluvial fans and alluvial valley-floor sediments from erosional rises, low hills and hills (Figure 4).

A detailed soil map was compiled by Stephens et al, (1945). Sixteen major soil types were recognised with most of the soils consisting of sandy loams, loams and clay loams with skeletal soils on bedrock slopes (Figure 5). The Belalie soil series is the most extensive and includes alluvial and colluvial sandy loams, loams and clay loams. Alluvial sediments were mapped east and south of Jamestown and over the south-east edge of the study area where they occurred as terraced deposits along valley floors.

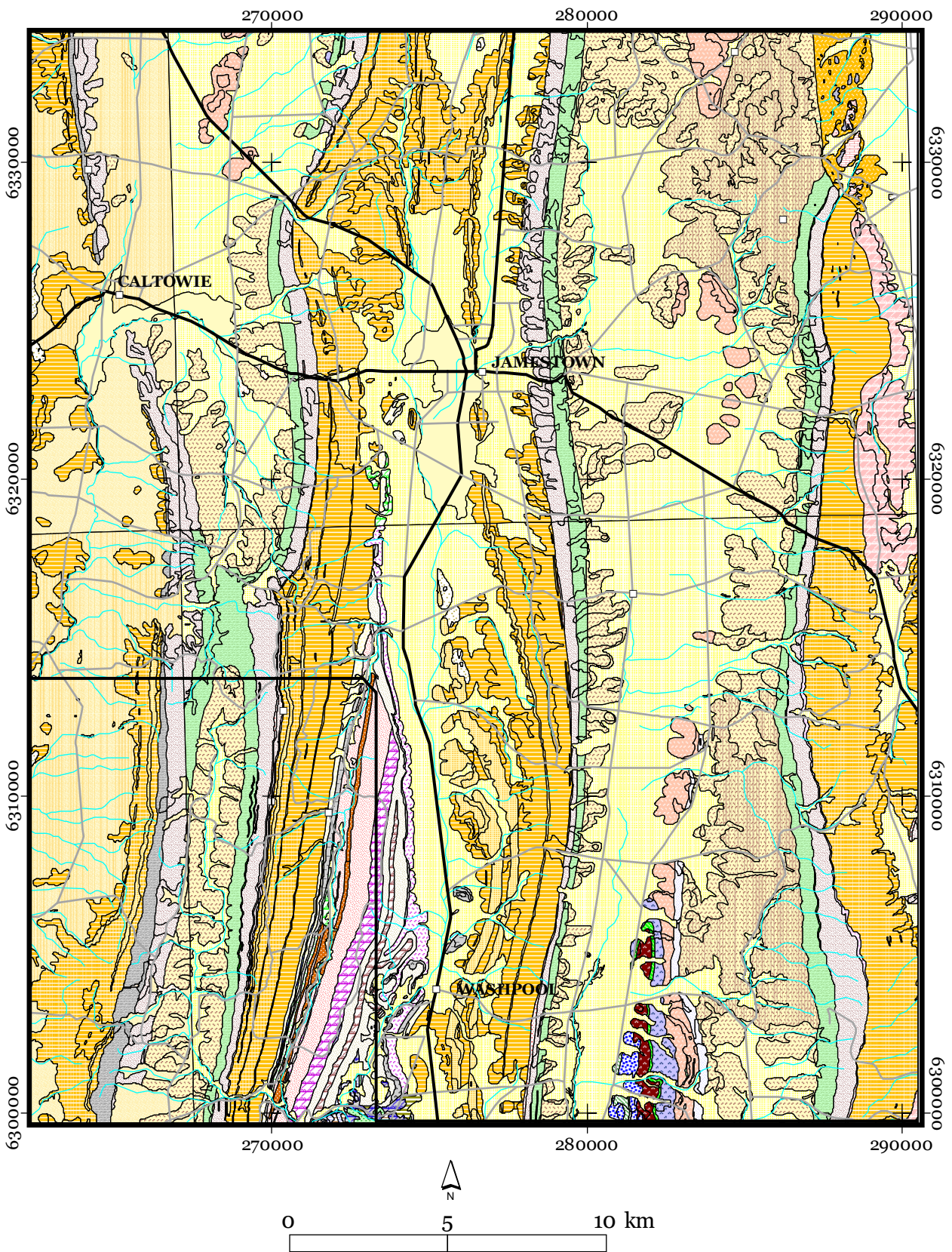


**Figure 2.** Geological map (Legend on next page). Some units have edge mismatches where different geological map sheets join.

	Alluvial plain sediments
	Clay, sand and carbonate earth, silty, with gravel lenses.
	Conglomerate, massive, well rounded pebble and boulder clasts, silty and sandy matrix; dolomite, massive to well bedded, grey and brown; breccia, dolomitic matrix.
	Dolerite in diapiric breccia. Based on green unit in Callanna Beds on ANDAMOOKA
	Dolomite
	Dolomite and dolomite marble, pale grey to cream; sandstone, interfingering at upper and lower margins
	Dolomite, blue-grey, cryptalgal-laminated. BURRA 2nd edition - preliminary unit for compilation
	Dolomite: BURRA 2nd ed. interim unit for compilation
	Dolomite; marble, with magnesite mud-pellet conglomerates.
	Dolomite; sandstone; siltstone; quartzite.
	Dolomite; siltstone; dolomitic limestone; sandstone; calcareous siltstone, basalt.
	Ferruginous pebbly grit, conglomerate, fine sandstone. Based on Ts on YARDEA
	Ironstone, ferruginisation, undifferentiated
	Lamprophyric intrusives, including kimberlite.
	Limestone or dolomite marble, cream, off-white, pale grey well-bedded, commonly finely sandy. BURRA 2nd ed. - interim unit for compilation.
	Limestone: BURRA 2nd ed. interim unit for compilation
	Lower member, typified by pale dolomite. BURRA: interim unit for compilation.
	Micaceous or talcose silty mudstone to v.f.g sandstone; white cherty siltstone; quartzite and dolomitic quartzite; BURRA 2nd ed. - interim unit for compilation.
	Mudstone; siltstone; shale, partly carbonaceous.
	Present day alluvium
	Quartz veins/bodies, undifferentiated
	Quartzite or sandstone interbeds.
	Quartzite, arenaceous, with conglomerate lenses.
	Quartzite, white to cream, medium-grained, well bedded, feldspathic; interbeds of sandy, carbonaceous and pyritic shale.
	Quartzite; arkose
	Quartzite; sandstone; siltstone.
	Sandstone and quartzite, interbeds. BURRA 2nd ed. - interim unit for compilation.
	Sandstone, arkosic.
	Sandstone, coarse-grained, feldspathic, conglomeratic.
	Sandstone, coarse-grained; sandstone medium to fine-grained, with siltstone.
	Sandstone, feldspathic, coarse-grained, commonly dolomite-cemented or with dolomite leached out; sandstone, fine to medium-grained; siltstone, grey.
	Sandstone, fine-medium grained, interbeds. BURRA 2nd ed. - interim unit for compilation.
	Sandstone, fine-medium, partly calcareous, interbeds. BURRA 2nd ed. - interim unit for compilation.
	Sandstone, progradational sand-wedge.
	Sandstone: BURRA 2nd ed. interim unit for compilation
	Sandstone; siltstone, grey; dolomite marble, grey and cream; dolomite, grey, flaggy, medium bedded, fine grained to coarsely crystalline; minor grey to black chert
	Shale, black; dolomitic siltstone; dolomite; grey laminated siltstone.
	Shale, pyritic, carbonaceous; thinly laminated grey dolomite beds and lenses.
	Siltstone and sandy siltstone, sparse granule to boulder erratics, pale grey or greyish green, massive or bedded, often calcareous. Minor lenses and interbeds of massive and laminated calcareous sandy siltstone and calcareous sandstone.
	Siltstone and shale, carbonaceous, black; sandstone and grit, fine to very coarse-grained, interbedded; dolomite, buff, partly stromatolitic, thin beds.
	Siltstone, blue-grey, thin bands of limestone and calcareous siltstone.
	Siltstone, dark grey, laminated with minor sandstone, dolomite interbeds; quartzite, fine to coarse, feldspathic, cross bedded, minor siltstone interbeds; slate
	Siltstone, green. Lower third is fine grained, includes glacial dropstones; middle unit is medium to coarse sandstone; upper unit is siltstone with minor sandstone. Minor diamictite, sandy and pebbly dolomite.
	Siltstone, grey to black, dolomitic and pyritic grading upwards to calcareous, thinly laminated, locally cross-bedded; dolomite, grey, laggy to massive; limestone conglomerate, intraformational; greywacke.
	Siltstone, locally carbonaceous; sandstone, locally stromatolitic, ripple marks, halite casts, heavy mineral lamination; carbonates; evaporites; basalt, minor acid and intermediate volcanics
	Siltstone, sandy, flaser bedded.
	Siltstone: BURRA 2nd ed. interim unit for compilation
	Siltstone; shale, green-grey and purple.
	Tillite; quartzite; siltstone. Massive, grey.
	Undifferentiated Quaternary rocks
	Undifferentiated alluvial/fluvial sediments
	Upper member, typified by dark dolomite. BURRA: interim unit for compilation.

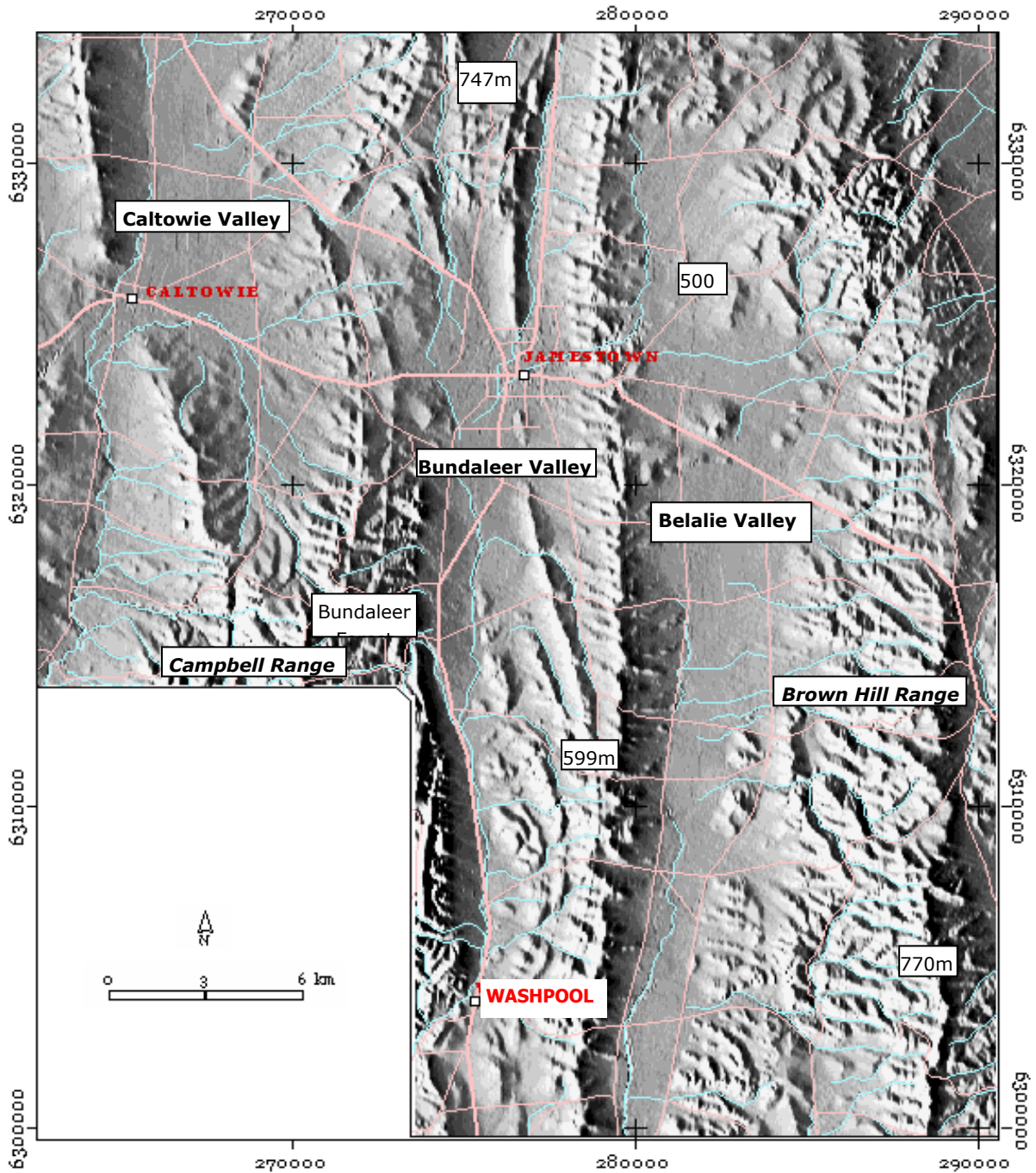


**Figure 3.** Hillshaded digital elevation model with roads, towns and surface drainage. Spot height elevations show relative changes in relief.

More recent soil landscape mapping (PIRSA, 2001) provides extensive information on soil characteristics and associated landform attributes. Soil-landscape units are defined principally from the interpretation of aerial photography and geology maps. Landforms delineated from aerial photographs are used as the principal surrogate when mapping soils because of the close genetic and spatial relationships between soils and landforms. Based on this approach, 23 major land systems are recognised in the area (Figure 6). These land systems are briefly described below.

*BAD Baderloo*

Alluvial flats and outwash fans of the Baderloo Creek Valley. Deep, mostly fertile and moderately well drained soils. Calcareous clay loams and loams common. Dryland salinity is a common feature effecting crop yields in this soil landscape unit.

*APP Appila*

Undulating rises and low hills formed on calcareous siltstone. Calcareous loams, clay loams and texture contrast soils common. Soils generally thin and susceptible to erosion.

*BBO Booborowie*

Alluvial flats and outwash colluvial fans of the Booborowie and lower Gum Creeks. Soil are deep and fertile but with poor surface structure leading to reduced water infiltration, compaction and water logging. Soils are typically hard loamy surfaces with red clay sub-soils.

*BLL Belalie*

Alluvial plains and gently sloping outwash fans of the Belalie Valley. Soils include red loamy textured contrast profiles with clayey sub-soils. Deep mostly fertile soils, although poor structure often leads to waterlogging. Minor saline seeps.

*BUN Bundaleer*

These include generally shallow soils (< 1 metre) associated with the Campbell Ranges and Bundaleer Hills. Lithosols and loamy soils with clay sub soils are common. Local valley flats consist of deep gradational sandy loams to clay loams and texture contrast soils.

*BUV Bundaleer Reservoir*

Landforms include rises and low hills with slopes mainly in the range of 4-20%. Loamy textured contrast soils are common. Shallow stony soils occur on steeper slopes and deeper gradational loams are best developed on alluvial flats. Gullying and scalding is a major feature of the land system.

*CNW Canowie*

Undulating rises, low hills and hills with mainly shallow loamy soils (calcareous in places) over basement rocks. Red clay sub soils common. Shallow stony soils on steeper slopes. Deeper textured contrast soils are common on lower lying sites.

*CTW Caltowie*

Alluvial flats, gentle slopes (outwash fans) and rises associated with the upper catchment of Yackamoorundie Creek and N/S of Caltowie. Texture contrast and gradational soils over alluvium and colluvium. Typically loamy textures with red clay sub soils. Shallow calcareous loams on rises. Minor saline seeps.

*GTN Georgetown*

Landforms consist of broad alluvial flats and outwash fans. Soils are characistically deep clay loams to cracking clays. Loamy texture contrast soils are common. Minor calcareous soils. Soils are generally fertile with minor limitation due to waterlogging, boron toxicity and salinity.

*KPW Kappowie*

Undulating rises and outwash colluvial fans west of Caltowie. Deep loams over clay and hard setting texture contrast soils on outwash fans and shallow calcareous loams on rises. Sediments typically mantled by fine windblown carbonate that has cemented to form calcrete.

*MDU Mundunnie*

Low hills, rises and outwash colluvial slopes with soils ranging from shallow calcareous loams and stony loams on upland areas to deeper loams over red clay on alluvial and colluvial sediments. Local scalding caused by high surface salt content or sodic subsoils (sub-soil salinity).

*MNG Mungcowie*

Generally shallow stony soils, where develop soils exhibit calcareous loam and red clay textures. Landforms are steep low hills on highly resistant tillites and quartzites.

*MNN Mannanarie*

Rises and gently inclined out wash fans. Minor steep rocky ridges. Soils include gradational loams, calcareous loams and shallow stony soils. Minor saline seepage commonly associated with low lying sites.

*MWA Mount Watts*

Moderately steep to steep hills with local prominent quartzite outcrops. Soils are generally shallow with well developed clayey subsoils. Shallow stony loams, calcareous loams and gradational loams are common.

*NBU North Bundaleer*

Landforms consist of rises, low hills, valley flats and minor rocky ridges. The main soils have sandy loam to clay loam textures, with soil depth ranging from shallow on rocky ridges to deep along valley floors. The land is an area of significant recharge to saline land lower in the catchment near Caltowie.

*NRN Narrien*

Moderately steep to steep ridges separated by undulating to gently rolling rises. Local relief varies between 30 to 150m. Most soils are loamy and shallow to moderately deep over saprock. On lower slopes the soils deepen and typically have red clay sub-soils.

*PIS Pisant*

Overall low relief consisting of rises and low hills. Soils include loamy to sandy loamy textured contrast and gradational soils with red clay subsoils. Isolated Tertiary remnants give rise to low fertile sandy soils.

*SPA Spalding*

Rises to low hills with slopes generally less than 10 %. Local colluvial fans on gentler slopes between rises and valleys floors. Most soils are deep over alluvium with loamy to clay textures. On rises soils are similar but shallower. Soils are often calcareous throughout.

*TEE Teetuppennie*

High relief landform consisting of hills and low hills. Most soils are shallow to moderately deep over weathered basement rocks. Shallow calcareous loams and lithosols are most common. Narrow alluvial soil along valley floors.

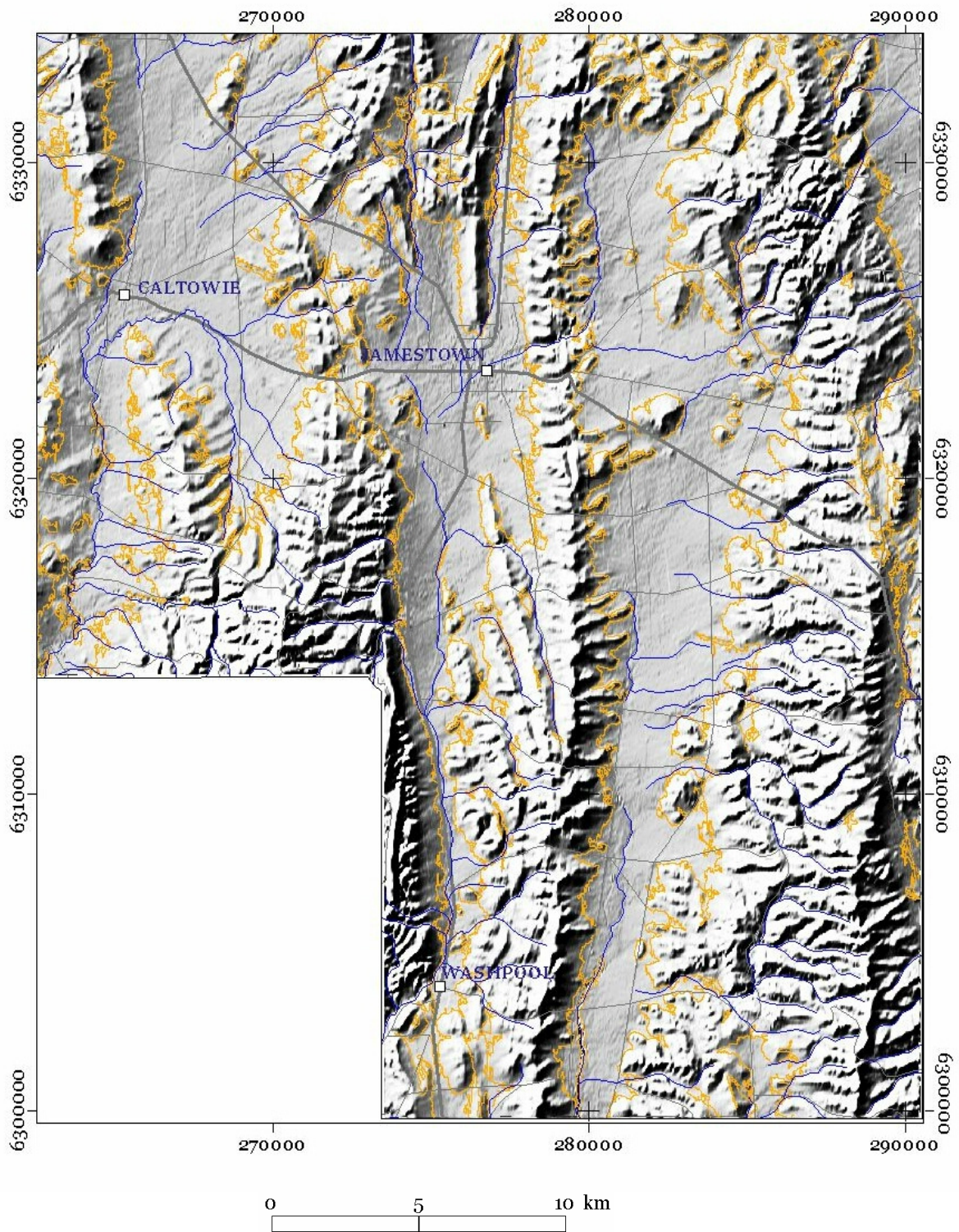


**Figure 4.** Hillshaded DEM with surface drainage in purple. The yellow line delineates slopes above and below 1.5 degrees and in most places separates erosional landforms ( $> 1.5$  degrees) from depositional landforms ( $< 1.5$  degrees).

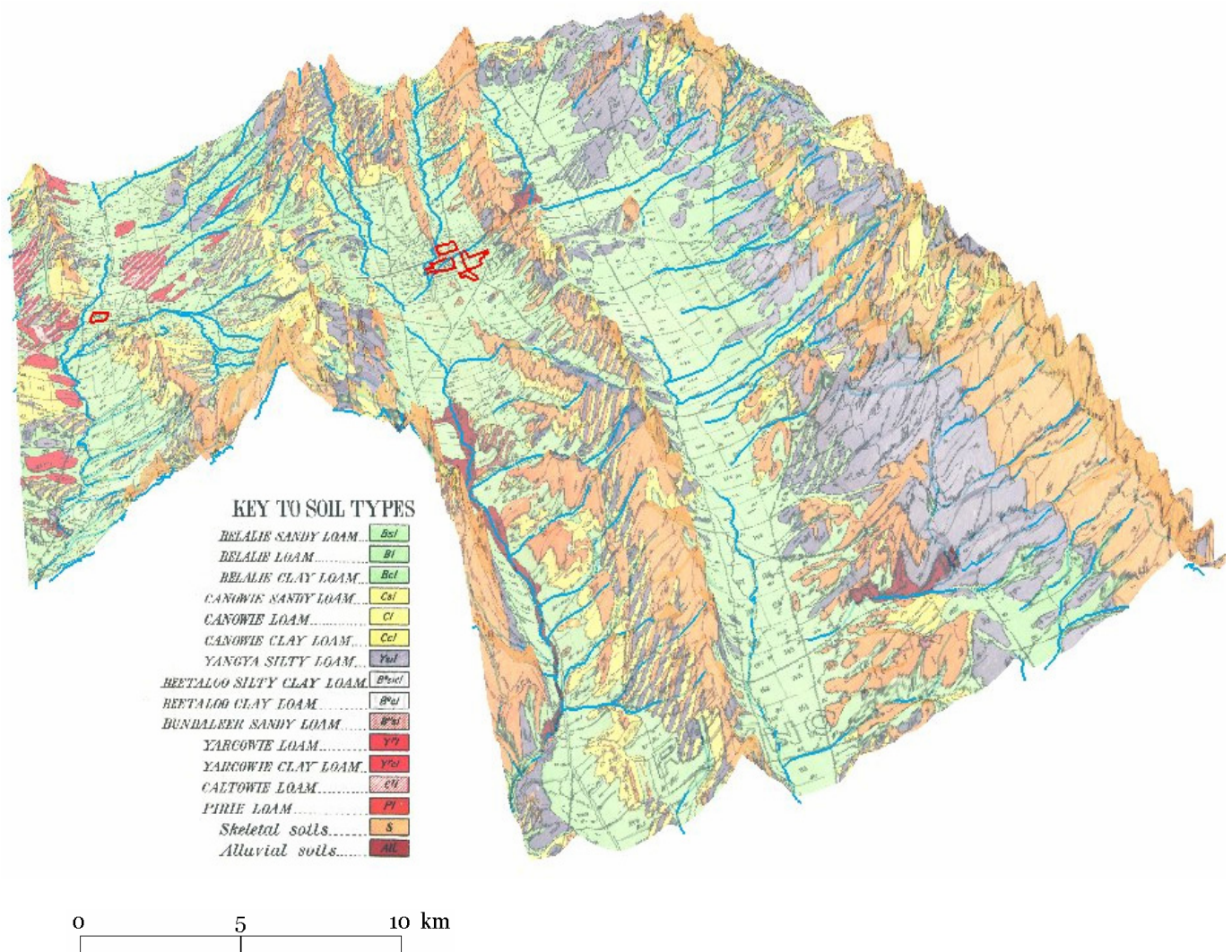


**Figure 5.** 3D perspective view of the 1945 soil map (Stephens, et al. 1945) draped over the digital elevation model.

#### WAP Wandre

Low relief alluvial and colluvial plains. Minor rises. Soils are characteristically deep with sandy to clays loam surfaces over red clayey subsoils. Shallower soils on rises. Texture contrast profiles are common.

#### WRD Ward Hill

Steep low hills, rises and minor valley flats. Resistive tillites, siliceous shales and quartzites form steep ridges. Soils are shallow calcareous and stony on upland areas and moderately deep to deep (red clay and loams) in lower relief areas. Salinity is restricted to local drainage depressions.

#### YCW Yarcowie

Landforms consist of alluvial flats and erosional rises. Most soils are deep over alluvial sediments and gentle slopes. Sandy loam to loam surfaces are common with red clayey sub-soils. Many of the soils are calcareous throughout. Shallow stony soils are minor.

#### YON Yongala

Landforms consist of rises, low hills, alluvial flats and gently inclined colluvial fans. Soils ranges from moderately deep loams to sandy loams with red clay subsoils in low relief areas to shallow calcareous loams on steeper hill slopes.

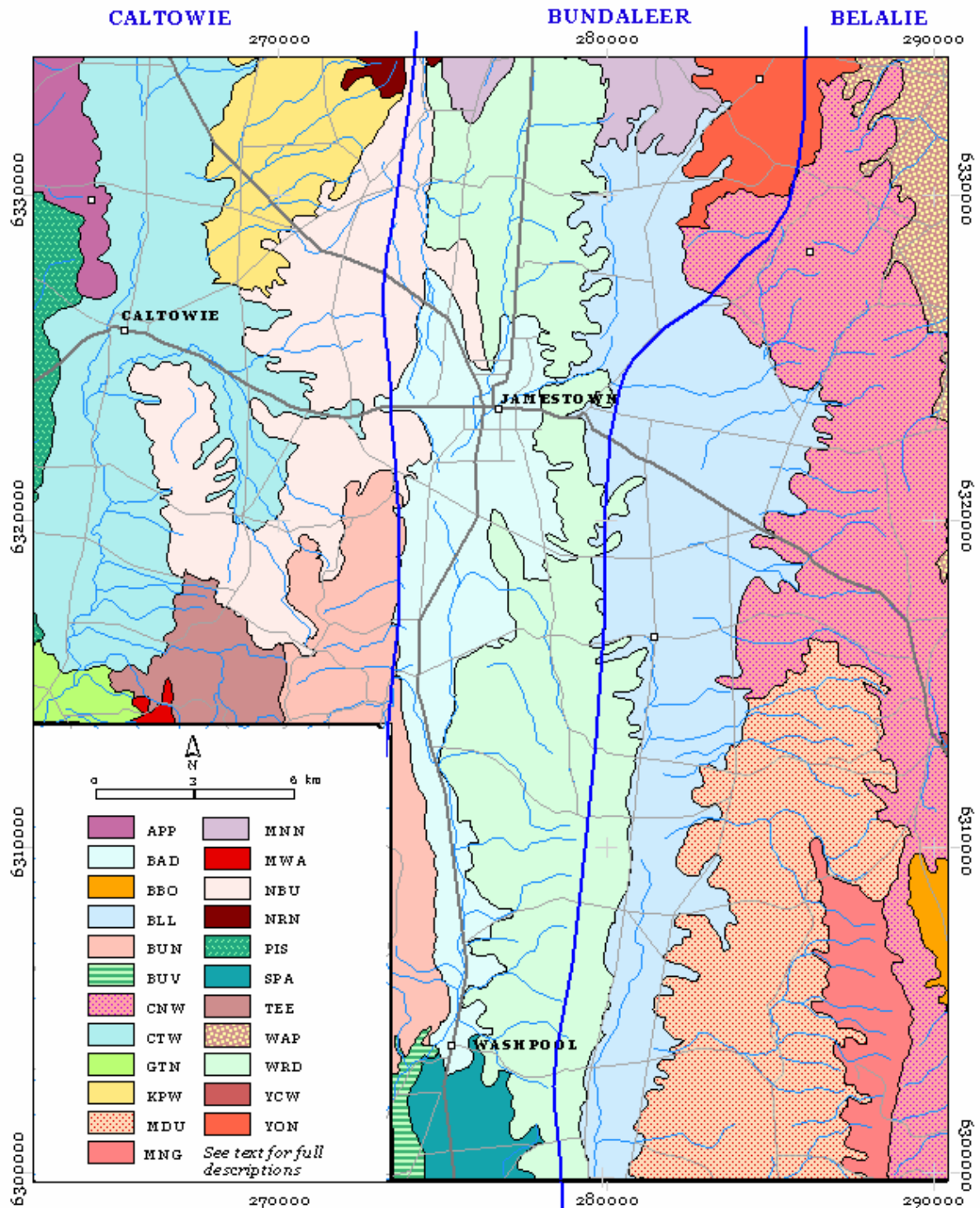


Figure 6. Major Soil Land Systems (PIRSA, 2001). See text for descriptions.

#### 4. HYDROGEOLOGY

##### 4.1 Origin of salt and dryland salinity

Stephens, et al., (1945), recognised salt scalds in the Jamestown area, but it was not until the 1970s that landholders recognised more extensive areas of dryland salinity associated with shallow groundwater tables (Henschke, et al., 1994). A hydrological investigation that included groundwater chemistry of a small catchment west of Jamestown (Henschke, et al., 1994) indicated that most of the ion species are characterised by chloride and sodium followed by sulphate and bicarbonate. The

accumulation of cyclic salts rather than bedrock weathering is likely to account for relatively high levels of Cl anions in the groundwater (Henschke, et al., 1994). A cyclic or rainfall origin for the chlorides is also supported from isotopic and chemical analyses (Cresswell and Herczeg, 2004). Measurements made from water bores show that total dissolved solids are higher in the valleys (up to 23356 mg/L) compared with the more elevated parts of the landscape (Figure 7). Areas of mapped dry saline land (PIRSA, 2001) occur in the Caltowie and Bundaleer catchments (Figure 7).

Several types of land salinisation occur in the region. The most important are:

1. Dryland salinity associated with shallow seasonal fluctuating groundwater tables within low lying alluvial and colluvial plains.
2. Root zone 'transient' salinity related to seasonal fluctuations of perched water tables (Rengasamy, 2002).
3. Salt induced scalds in upland areas (steep slopes and ridge crests) sometimes referred to as 'magnesia patches'. Although many of these scalds may, in fact, be erosional features caused by over grazing.

## **5. STUDY METHODS – data acquisition and processing**

### **5.1 Gamma-ray spectrometry and magnetics**

Gamma-ray spectrometry and magnetic data were collected by Fugro Airborne Survey during June-August 2002 using a flight-line spacing of 100 metres and a nominal terrain clearance of 60 metres. An Exploranium GR-820 spectrometer and a geometrics G822A magnetometer collected the gamma-ray and magnetic field dataset, respectively. All data are presented using the GDA94 datum within MGA zone 54. The following coordinates define the survey area; 263000E 6334000N:290000E 6334000N:290000E:630000N : 274000E:630000N and 274000E:6314000N.

#### **5.1.1 Gamma-ray spectrometry**

Gamma-radiometrics measures the natural radiation from potassium (K), thorium (Th) and uranium (U) in the upper 30cm of the earth's surface. Potassium is measured directly from the decay of  $^{40}\text{K}$ . Thorium and U are inferred from daughter elements associated with distinctive isotopic emissions from  $^{208}\text{Tl}$  and  $^{214}\text{Bi}$  in their respective decay chains, so they are usually expressed in equivalent parts per million eU and eTh. Potassium is more abundant and is expressed as a percentage. Gamma-rays were detected using a 50.3L NaI (T1) crystal pack across 256 channels. A series of data processing and calibration steps were then performed including NASVD noise reduction or spectral smoothing (Minty 1997), cosmic, aircraft and radon background removal, stripping and height corrections. For detail descriptions of flight acquisition and data processing steps, refer to Fugro Airborne Surveys Pty. Ltd technical report (2002a). The flight-line data were micro-levelled for each band and a minimum curvature algorithm was applied to produce grids with 20 m cell size.

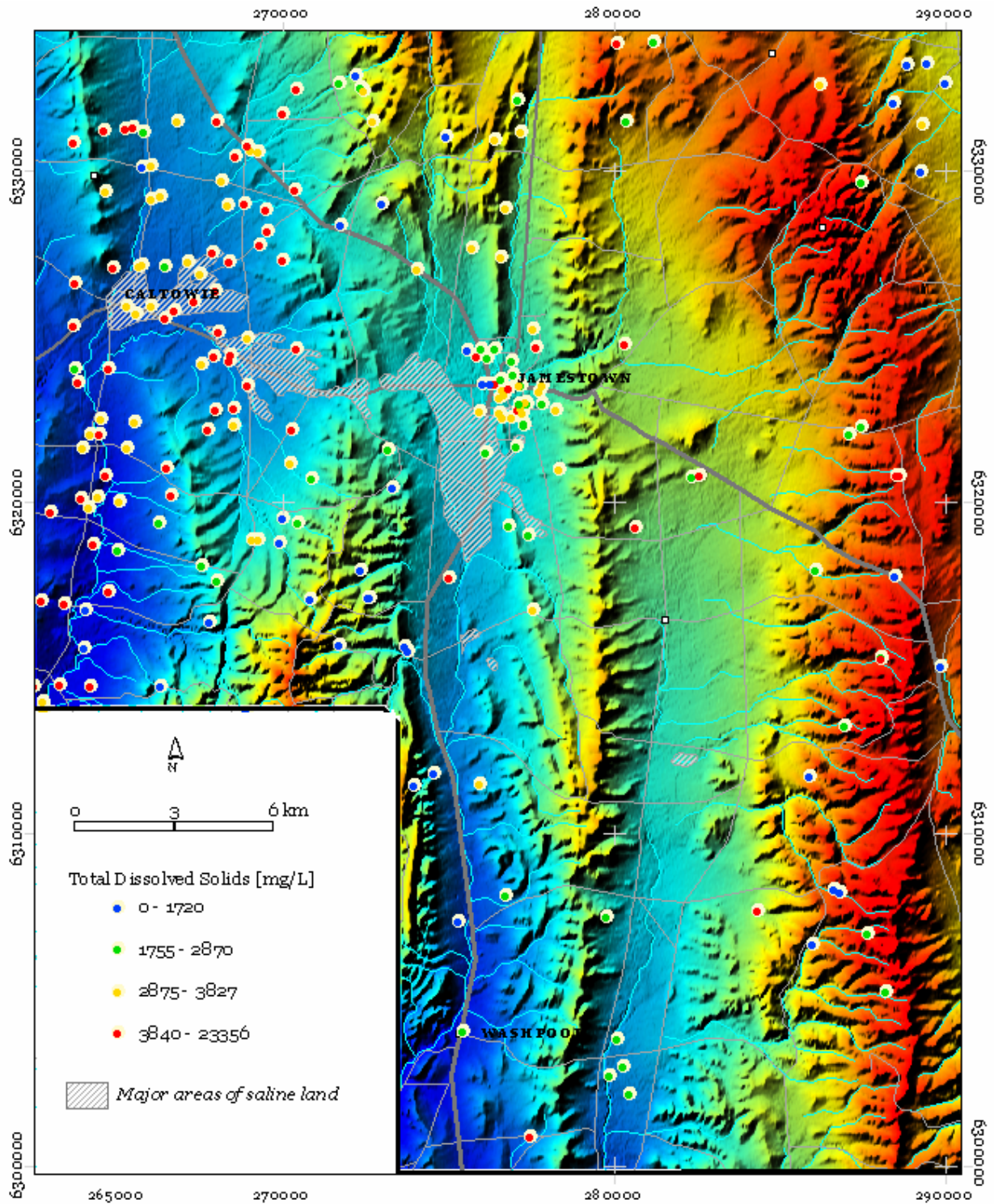


**Figure 7.** Areas of dryland salinity and TDS concentrations from bores.

Gamma-ray grids were displayed either as single pseudo-coloured images with red to blue colours relating to high and low gamma-ray values respectively, or as three band colour composite images with potassium in red, thorium in green and uranium in blue (Figure 8). Images were enhanced with ERmapper software and integrated as raster images within the 3D modelling environment of GOCAD

software. Gamma-ray radiation emitted from the ground surface (to a depth of approximately 30cm) reflects the chemical composition of the bedrock, regolith and overlying soil. Gamma-ray imagery therefore shows geochemical variations of K, Th and U in exposed regolith and bedrock.

### **5.1.2 Magnetics**

The magnetometer recorded signals at approximately 7 m intervals along each flight-line with a sensitivity of .001nT. A line-spline algorithm was used to produce gridded magnetic data with 20 m cell size resolution for enhancement and display in ERMapper and later modelling and integration with other datasets using ESRI-ArcInfo GIS and GOCAD software. First vertical and horizontal derivatives of the magnetics were produced to highlight major lithological, structural and high frequency features in the data. The high frequency component of the magnetic image was specifically enhanced to highlight the presence of any near-surface regolith magnetic material (eg. maghemite gravels).

## **5.2 Digital elevation model**

A digital elevation model is calculated from the aircraft using Global Positioning System (GPS), altitude (flying height - ASL) and a radar altimeter (flying height above the ground). Elevation measurements were collected at 60 m intervals along each flight-line. There was 100m between flight-lines. Tie line levelling and further micro-levelling along each flight-line produced the final levelled terrain model. A line-spline algorithm was also used to produce gridded data with a 20-metre cell size for the survey area (Fugro, 2003). The survey size is the same as defined for the gamma-ray spectrometry survey.

The elevation models were processed to derive a series of surfaces that described major geomorphological, structural and hydrological characteristics in the study area. Primary terrain attributes including slope, aspect, elevation and hillshaded relief images were generated from the DEM data to describe major landform elements. Digital elevation model derived hydrological surfaces and attributes included catchment boundary delineation, drainage networks, stream ordering and stream gradients. Digital elevation models also had an important role in allowing more effective landscape visualisation. For example combining gamma-ray spectrometry images with terrain models as 3D perspective drapes facilitated the visualisation and understanding of the relationships between gamma-ray responses and surface morphology.

## **5.3 Airborne EM**

Airborne electro magnetics measures the electrical properties of the sub-surface potentially down to two hundred metres. Fugro Airborne Surveys (2002b) flew the Jamestown survey with the TEMPEST™ system between 22<sup>nd</sup> July and 27<sup>th</sup> July 2002. A total of 1,404 line kilometres were flown with a flight-line spacing of 400m. Specifications of the TEMPEST Airborne EM System are described by Lane et al., (1999). A bicubic polynomial gridding routine was used to generate an 80 m

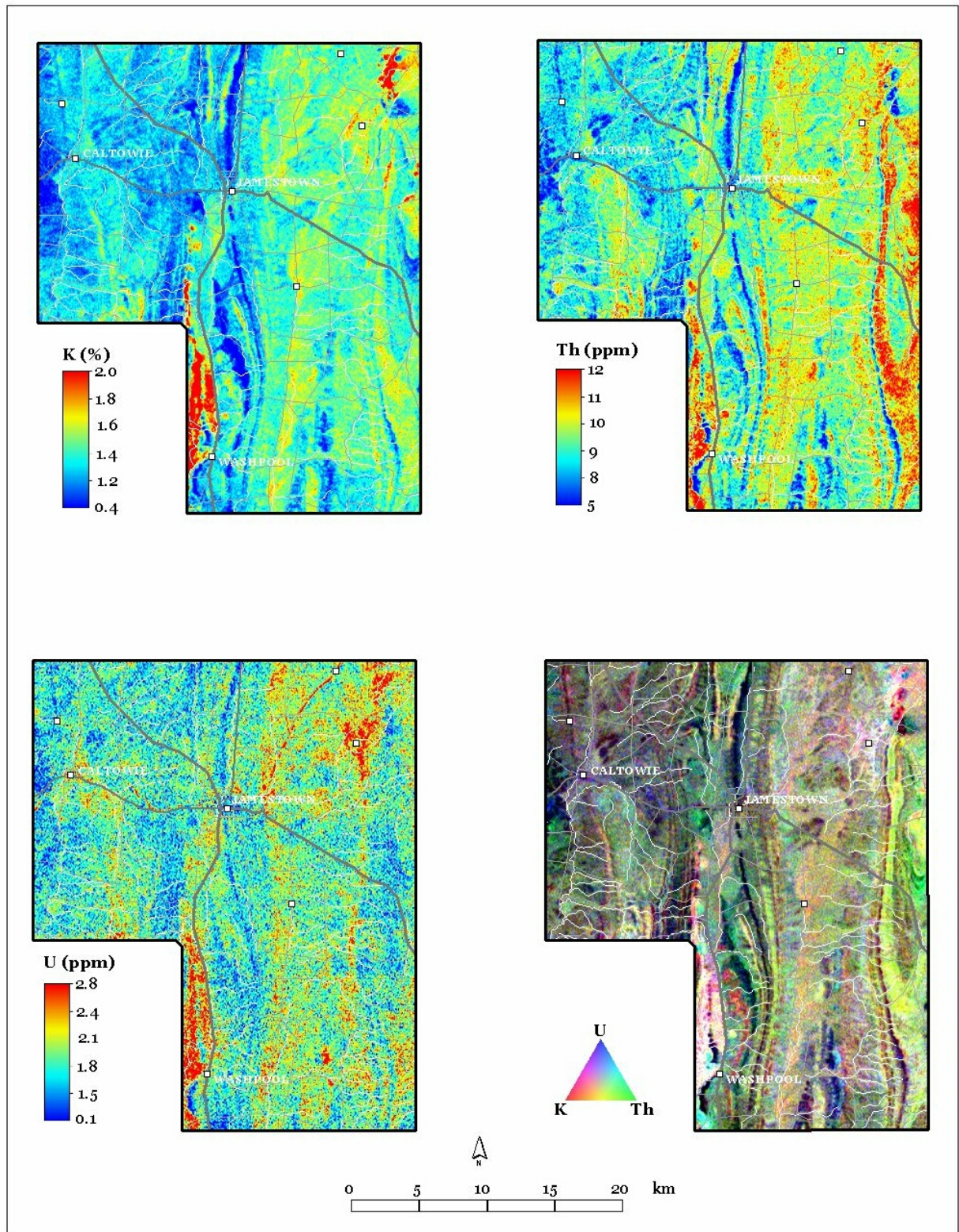


**Figure 8.** Pseudo-coloured and three band false colour composite image of K, eTh and eU.

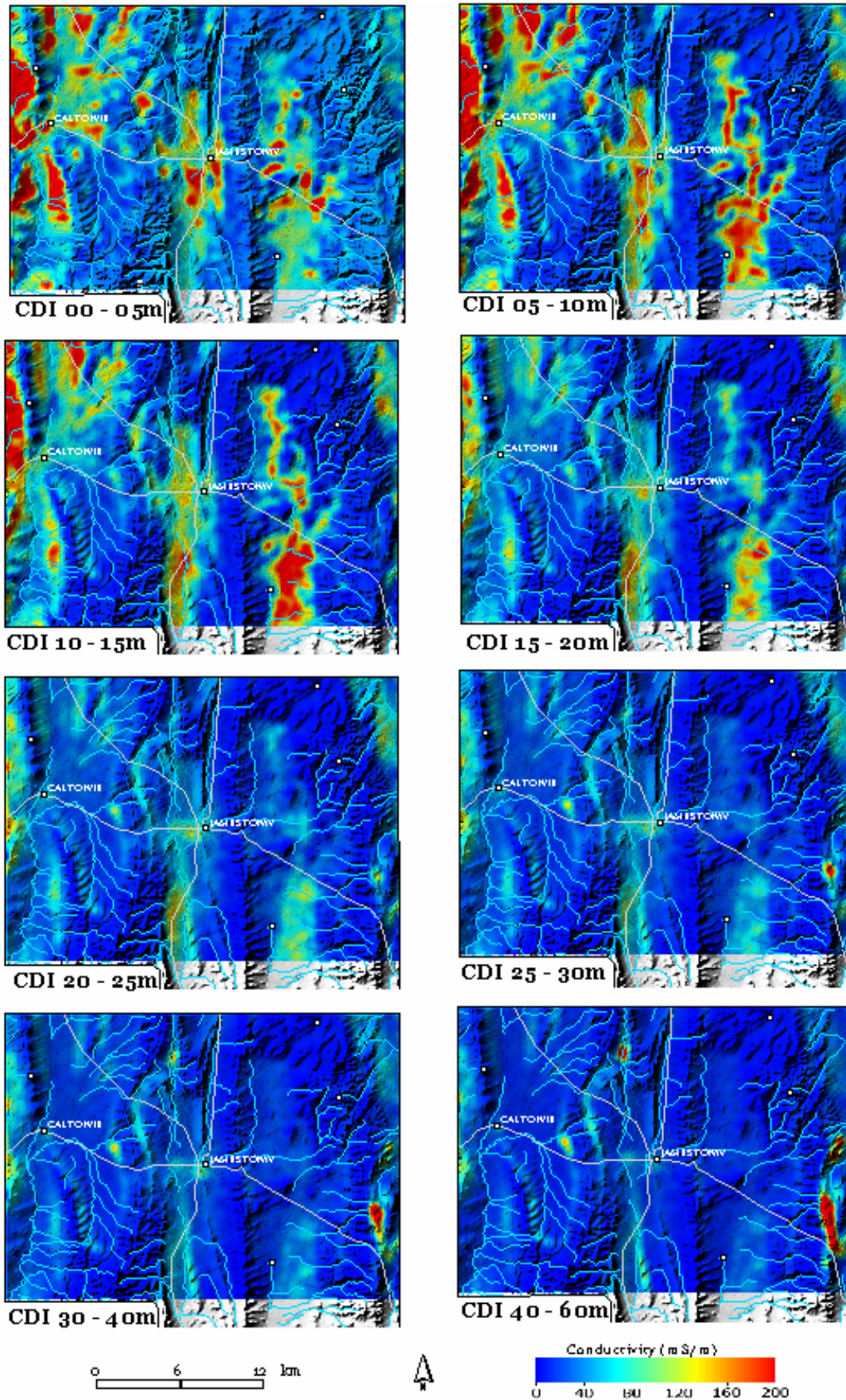


**Figure 9.** Conductivity depth image (CDI) slices with hillshaded DEM and drainage attributes added. All image scale from 0 – 200 mS/m. (processed by Fitzpatrick, 2003)

grid cell size from the 400m flight-line data (i.e. 1/5 the line spacing). Acquisition parameters and processing steps involved in the TEMPEST system are described in Fugro report (2002).

To enable easier interpretation, the processed AEM window amplitude data were inverted to determine the sub-surface electrical conductivity. This was done using the conductivity depth imaging or CDI method (Macnae *et al.*, 1998). Conductivity depth interval (CDI) sections for TEMPEST data were calculated using EMFlow (Figure 9). The method assumes the earth consists of uniformly conductive horizontal layers. Each observation along the flight lines is transformed or inverted separately, and the derived conductivities are then “stitched” together to form the 3D sub-surface conductivity distribution. The derived conductivity distributions were used to generate interval conductivity images at 5m depth increments below the surface. Conductivity depth information was also imported into the GOCAD 3D modelling software. This allows 3D integration with other datasets such as drill hole logs and the creation of iso-surfaced (3D surface of equal value) conductivity volumes (Lane *et al.*, 1999, Wilford, 1999).

#### **5.4 Drill hole information and surface soil sampling**

Sub-surface information on regolith properties were obtained from the interpretation of existing drill logs and newly acquired drill hole samples and logs (Jones and Henschke, 2003). A sub-set of existing drill logs were selected to represent the range of regolith materials in the region. Locations of these drill holes are displayed in figure 10. Several broad classes of regolith, including transported and *in situ* weathered materials were reinterpreted from the driller’s logs (Figure 11). Where possible, alluvial or colluvial materials were then separated and the degree of bedrock weathering estimated (eg. very highly weathered saprolite through to saprock or slightly weathered bedrock) based largely on bedrock texture, particularly the percentage of weathered clay and degree of mottling. The regolith classes used to describe the drillholes include:

1. Alluvial and colluvial clays, silts and minor gravels
2. Alluvial clay/silt and minor gravels
3. Colluvial clay/silt and minor gravels
4. Residual clay with minor gravels
5. Highly weathered saprolite (typically high clay content)
6. Mottled saprolite
7. Moderately weathered bedrock
8. Saprock (bedrock structure and mineralogy largely unchanged)
9. Saprock to fresh bedrock

Drill logs reported by Henschke, et al (2003) assisted in describing the characteristics of the sediment valley fill deposits including texture, composition, weathering characteristics, salt load (based on 1:5 ECs) and depth of sediments. The logs described by Henschke et al (2003) were also reinterpreted into major regolith classes as described above. Both sets of drillhole datasets were used in interpreting the AEM dataset and in characterising the valley fill materials (see section 6.0).

Soil samples were collected to assist with the interpretation of the airborne gamma-ray spectrometric datasets. Soil samples were analysed for particle size using a Malvern Mastersizer 2000 laser diffractometer ([http://www.malvern.co.uk/malvern/rw\\_malvern.nsf/vwa\\_docref/MS2K+PP](http://www.malvern.co.uk/malvern/rw_malvern.nsf/vwa_docref/MS2K+PP)). A representative, stratified soil sampling approach was developed to insure soil samples were collected from a range of gamma-ray responses and landscape types. This was done by generating an unsupervised classified image that used slope from the DEM and the K and Th bands. The Uranium band was not used in the classification due to its relatively high noise content. Eight classes were generated and a minimum of 8 soil samples were collected from each class (Figure 12). Standard linear correlation methods were then applied to assess whether correlations existed between gamma-ray response and soil texture.

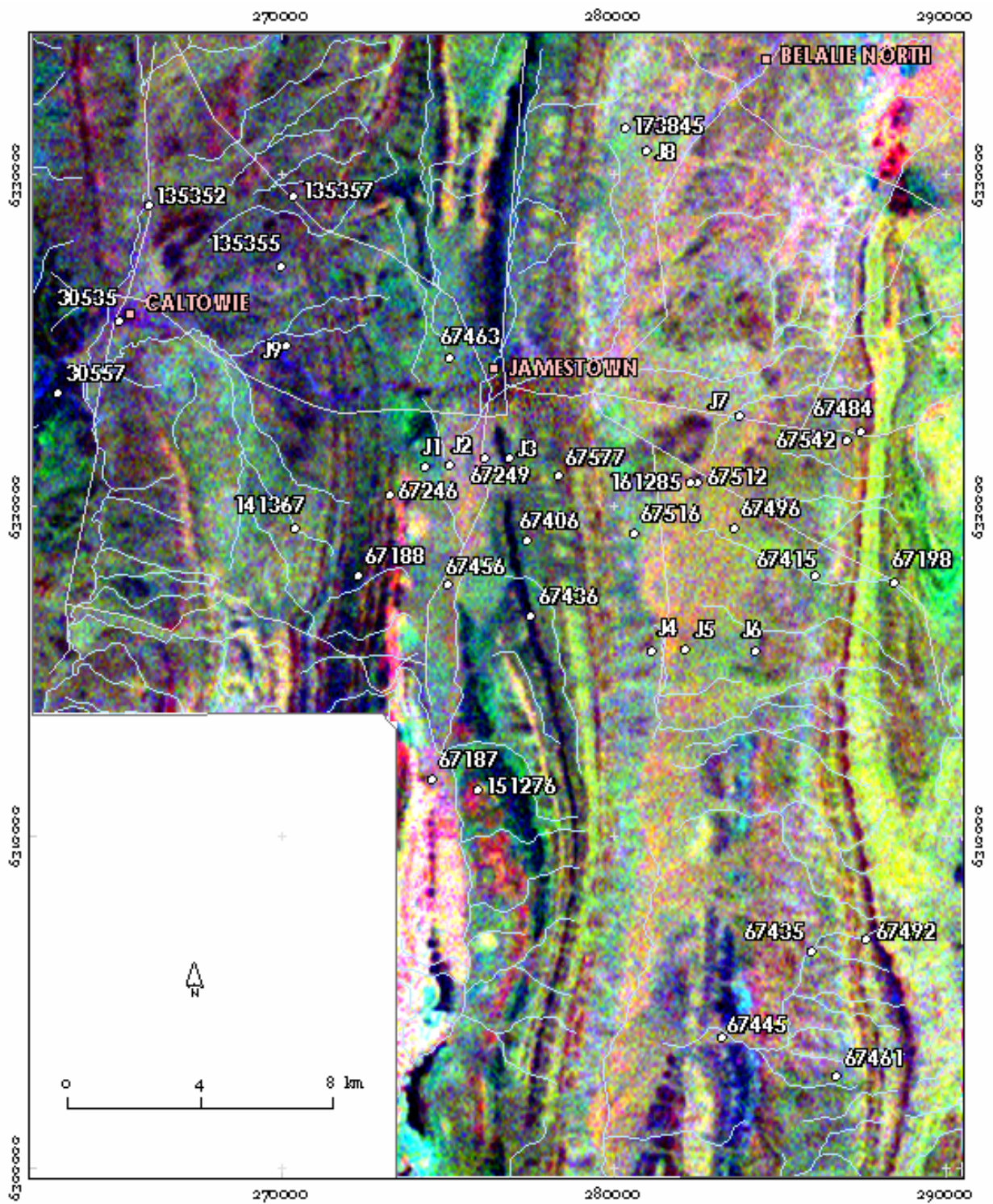
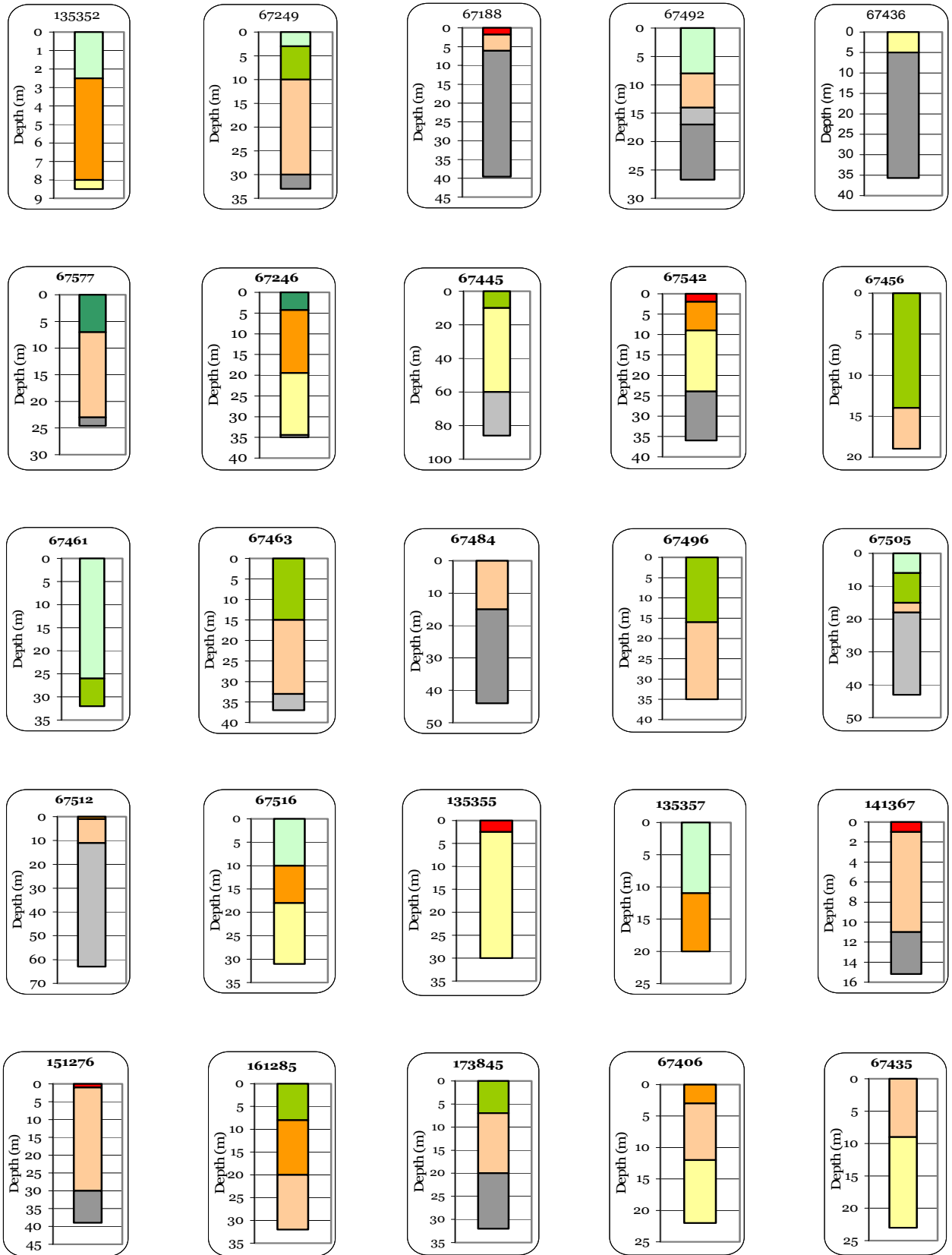
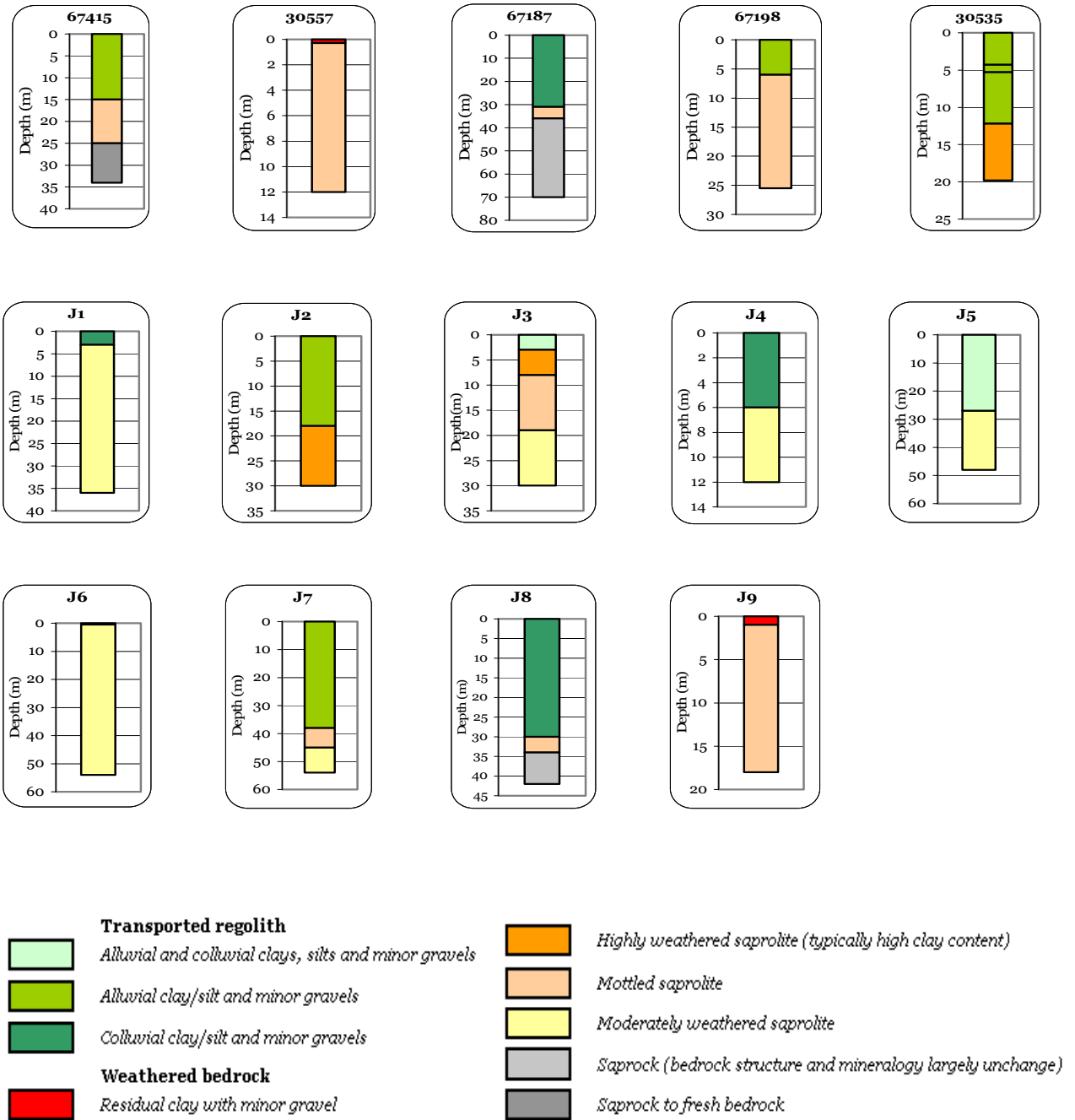


Figure 10. Location of interpreted drill holes.



**Figure 11.** Interpreted drill hole sections



**Figure 11.** Interpreted drill hole sections and drill log key

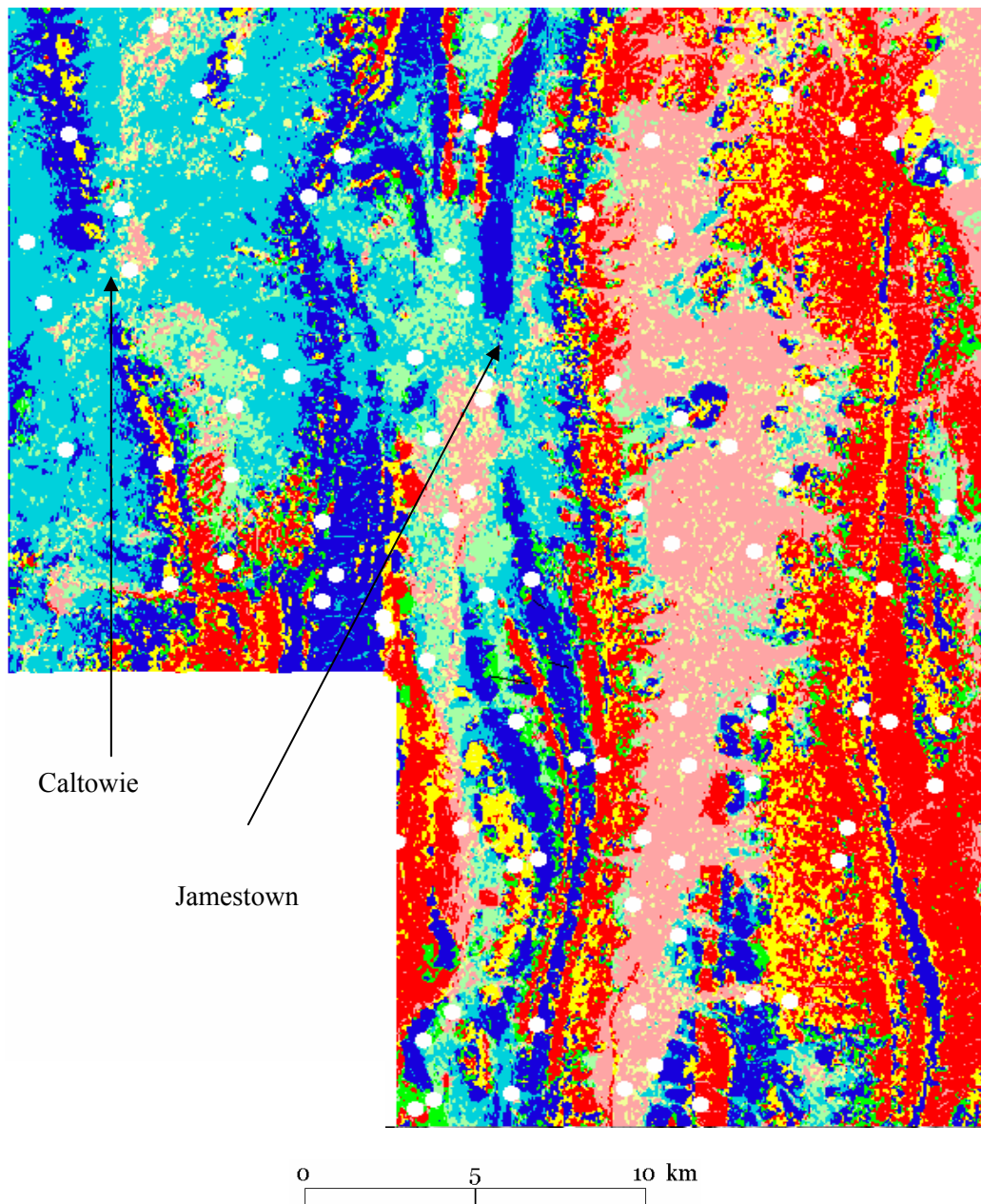


**Figure 12.** Location of surface soil samples used to characterise the gamma-ray response. Unsupervised classification of the K, eTh and slope was used to stratify surface soil sampling. This allowed samples to be collected that reflected a range of landform and gamma-ray responses. The Uranium channel was not used in the classification because of its higher noise content.

## 5.5 Ground geophysics

### 5.5.1 EM31

The EM31 measures apparent conductivity of the upper 3-6m of the regolith. Conductivity depends on soil moisture, soluble salts, temperature, texture (particularly the clay content) and the nature of the parent material (eg. presence of magnetic minerals). However, most of the variation seen in EM31 logs relate to the soil moisture and salt content. EM31 surveys have been used extensively in mapping salt affected land and shallow saline ground water tables based on the relationship between high conductivity and salt content in the upper part of the regolith. However, it should be recognised that there is not always a direct correlation between high EM responses and salt concentrations. For example, soils with high clay content and cation exchange capacity can be more conductive than sandy textured soils with similar salt concentration. Therefore where there are major variations in soil texture

across the survey, calibration coefficients should be used to estimate the effects of soil moisture when estimating salinity.

In this study EM31 transects were used as a guide to map clay-rich regolith materials and salts in the upper 3-6 m of the weathering profile. The EM31 transects assist in validating thematic regolith maps generated from interpreting the airborne gamma-ray spectrometry imagery. EM31 measurements were collected at 20 to 40 m intervals along the transects depending on the local variability in the landscape (relief and regolith). These transects were surveyed orthogonal to streams or valley floors to intersect a range of materials from hill slopes to valley sediment (e.g. colluvial and alluvial).

## 6. RESULTS

### 6.1 Interpretation of airborne spectrometry.

#### 6.1.1 *Gamma-ray response of bedrock and regolith*

Gamma-rays emitted from the surface will relate principally to the mineralogy and geochemistry of the bedrock and weathered materials (eg. soils, saprolite, alluvial and colluvial sediments). In erosional landscapes (i.e. rises, low hills and hills) with exposed bedrock and shallow soils the gamma-ray response largely reflects differences in bedrock chemistry. Siliceous tillites and quartzites that typically form resistant ridges appear black in the ternary image due to low count for each of the 3 radioelements (typically ranges – K 0.8-1.0 %, Th 5-7 ppm and U 0.9-1.7 ppm) (Figure 8 and 13). Generally the higher the silica content of the lithology, the lower the overall gamma-ray counts. High radioelement counts, particularly K, are associated with felspathic sandstones, micaceous siltstones and local outcrops of acid to intermediate volcanics (typical ranges: K 2.0-4.5%). Siltstones, including some calcareous siltstones, mudstones and dolomites, have relatively high Th (11-16ppm). The uranium channel data are noisy with its speckled appearance making it difficult to interpret. However, relatively high values are associated with felspathic sandstones, micaceous siltstones and local acid intrusive rocks.

Gamma-ray responses of sediments associated with flood plains, colluvial and alluvial fans are also variable. This variability partly reflects the diversity of materials from which the sediments have been derived, modifications of surface geochemistry due to weathering and grain size sorting as a result of sheet flow and channel processes. A 1.5-degree slope boundary line effectively separates most of the colluvial and alluvial fan deposits (ie. < 1.5 degrees) from bedrock responses on rises and hills (i.e. > 1.5 degrees) (Figure 13). Higher K and to a lesser extent Th values are associated with sediments in the Belalie and Bundaleer catchments compared with sediments in the Caltowie catchment. These values reflect textural and compositional differences between the catchments. Preliminary grain size analysis using a laser grain size determination method for surface soil samples showed a significant correlation ( $r^2 = 0.6$ ) between airborne K concentration and silt content. Higher K values correlated with higher silt content in surface soil (Figure 14). The relationship is only based on samples that are equal to or below 1.5 degree slopes. This effectively isolates the transported valley-fill sediments from bedrock K responses. Plots for airborne K verses silt showed poor correlations for the whole sample population that included both thin soils on bedrock and sediments. The regression line for the K verses silt plot was then used to predict silt content within each of the three major catchments. The Belalie, and to a lesser extent the Bundaleer, depositional plains had much higher silt contents than sediments in the Caltowie catchment (Figure 15).

The high silt content of the Belalie catchment is likely to reflect the abundance of phyllitic and siltstone lithologies within the drainage basin. This could not be predicted using the geology map alone, since most of the bedrock units contain a range of lithologies (e.g. the bedrock units are

undifferentiated containing - siltstones, sandstones and mudstones). The highest K values also appear to be associated with channel depressions and stagnant drainage lines with very low gradients. This suggests that the silts were deposited from suspension in flood plain or sheet flood fan environments. Based on X-Ray Diffraction (XRD) analysis on the high and low K response soil samples the elevated K is associated with silt size mica (muscovite) and illite grains, whereas, low K soil samples have a higher proportion of quartz and low mica/illite content. A significant proportion of the silts might be derived from reworking of aeolian dust mantles over the region. The dust would have accumulated under dryer climatic conditions than the present day and similar to those described by Butler, 1982, Chartres et al. 1988, and Chor et al. 2003 and Williams, et al. 2001).

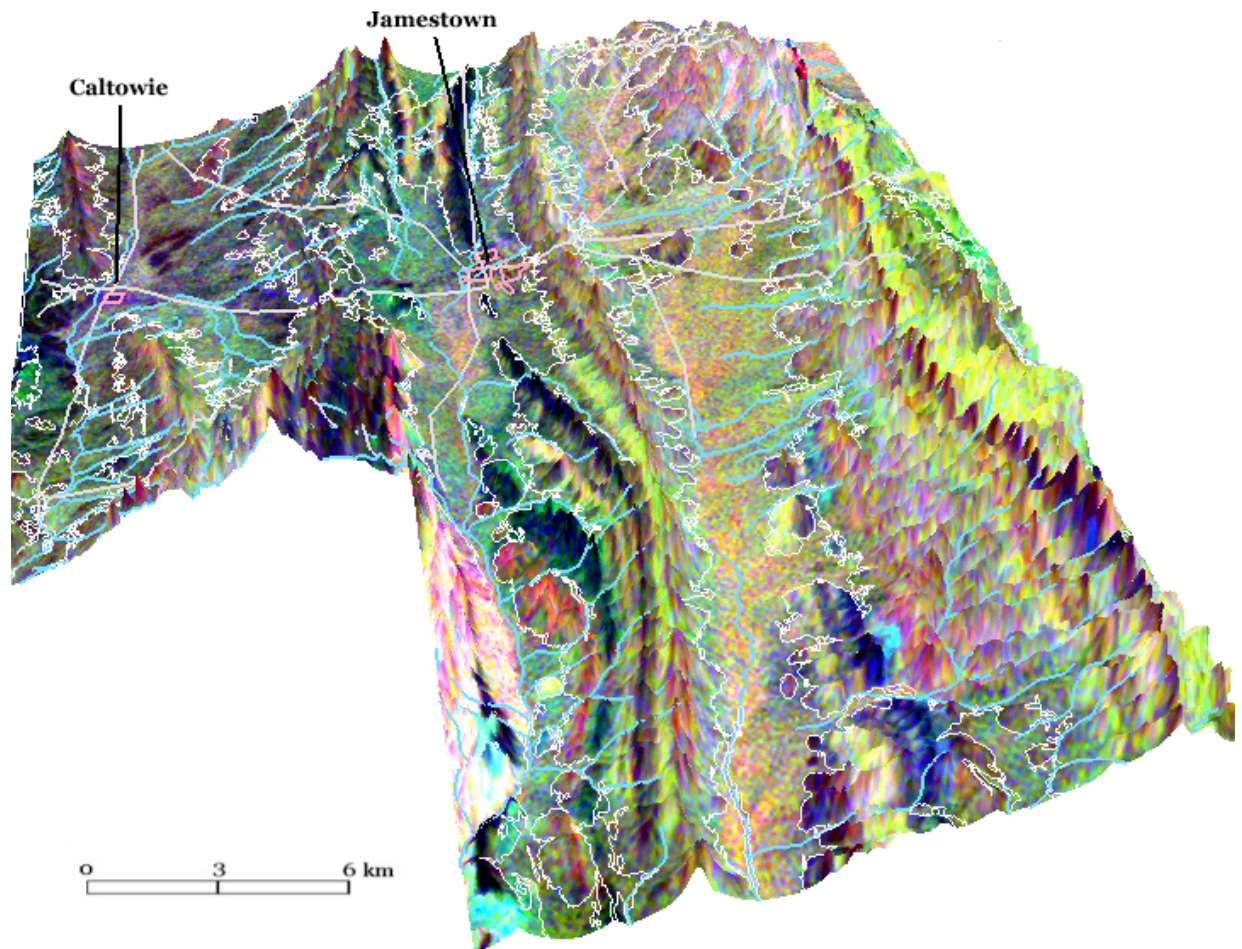


**Figure 13.** 3D perspective drape of 3-band gamma-ray spectrometry image over the digital elevation model. The white line delineates slopes above (erosional landscapes) and below 1.5 degrees (depositional landscapes).

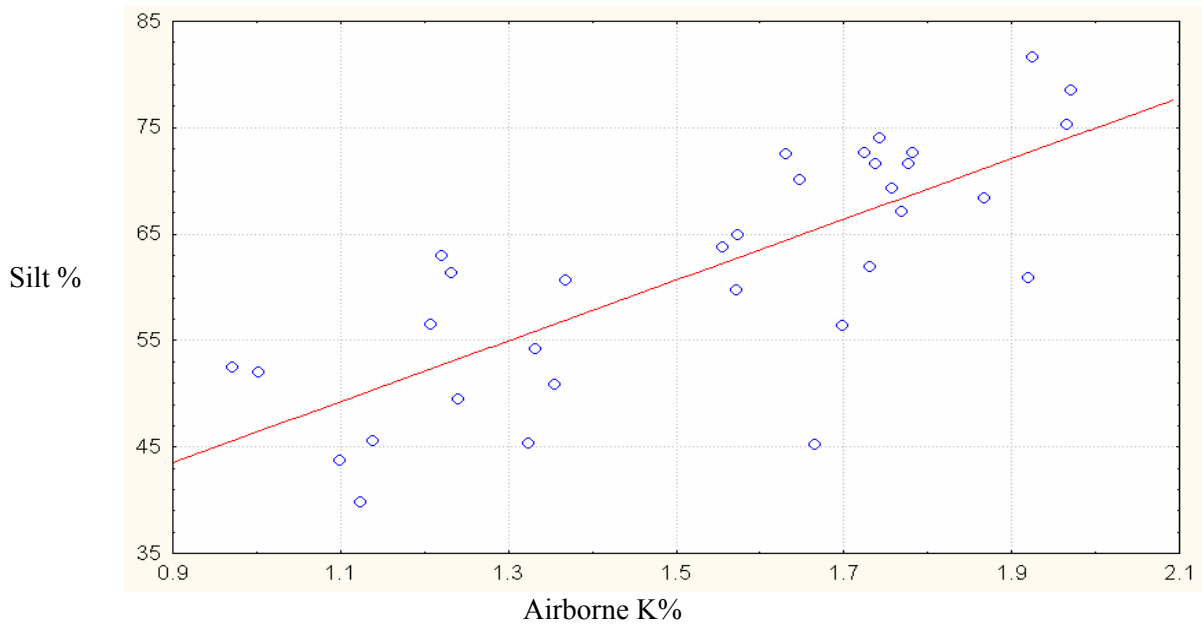


**Figure 14.** Relationship between surface soil silt content and airborne K concentration. Samples plotted for deposition landscapes only.  $R^2 = 0.6$

Therefore, soils in the Caltowie catchment are generally sandier with a higher proportion of fine sand. The pattern with Th is less clear. The relative high Th content of the Belalie sediments compared with those in the Caltowie valley probably reflects the higher Th content of rocks within the Belalie catchment. Interestingly, there is not much differentiation of Th concentration within either of the valley systems. Thorium might be associated with a range of grain sizes (e.g. fine sand, silt and clay) and as a consequence is not easily separated or concentrated within depositional plains.

A series of distinct colluvial fans are recognised on the eastern flank of the Bundaleer Range (Figure 16). The fans are characterised by having high K, Th and U or low K and high Th and U. The rocks contributing sediment to these fans have high radioelement counts for each of the three radioelements. Fans with similar gamma-ray signatures to that of the parent bedrock are likely to have been actively eroded and deposited. These active fans still retain their bedrock signatures. Whereas fans with low K, suggests weathering or leaching of K-bearing minerals and likely retention of Th and U where they might be associated with resistate minerals, clays and iron oxides. These fans are less active with relatively low geomorphic rates.

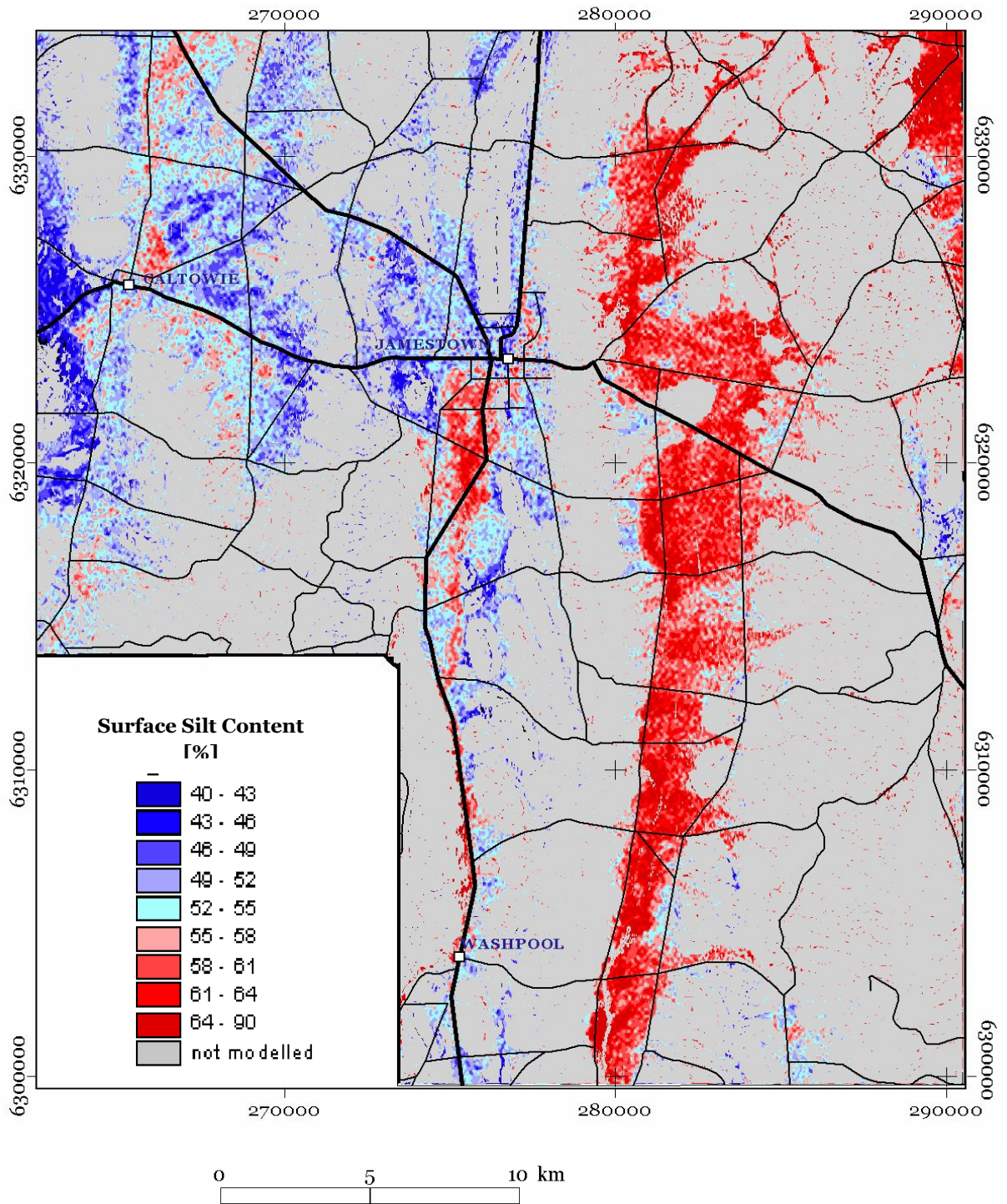


**Figure 15.** Modelled surface soil silt content based on the correlation between airborne K and silt. The Belalie and to a lesser extent Bundaleer depositional plains have significantly more silt than the Caltowie catchment.

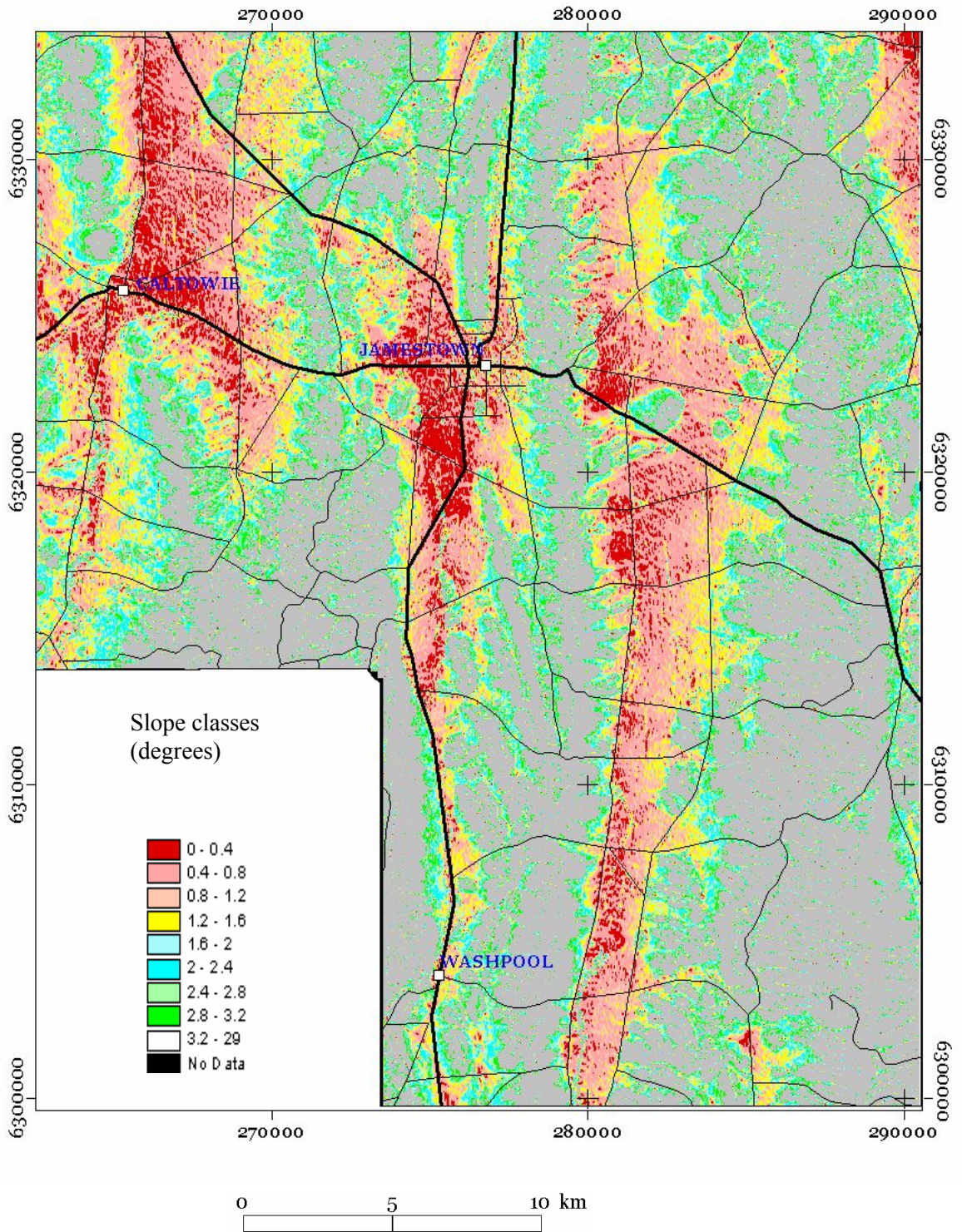
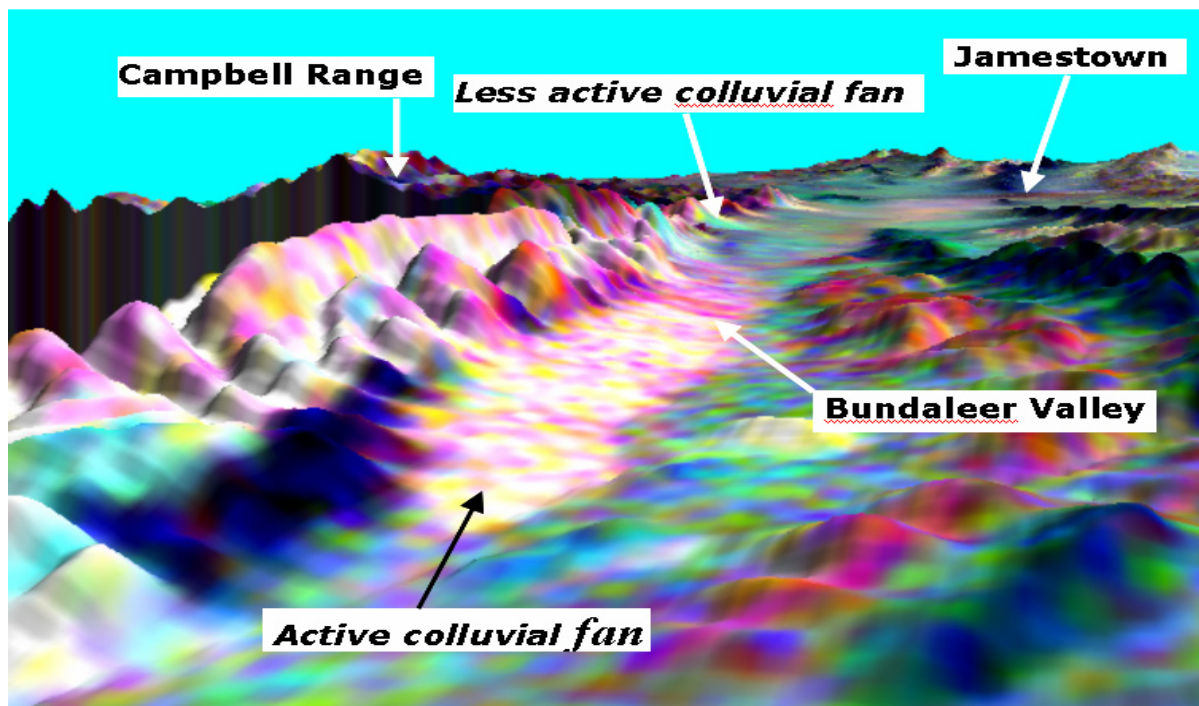


Figure 17. Slope map derived from the DEM.



**Figure 16.** 3D perspective image of the 3-band gamma-ray draped over the digital elevation model. Colluvial fan developed along the east edge of the Bundaleer Range are highlighted. Rocks contributing sediment to these fans are high in each of the three radioelements. Active fans have similar radioelement signatures to that of the bedrock - inactive fans have lost K due to mineral weathering and leaching. These fans appear in blue/green tones reflecting relatively high eTh and eU compared with K.

## 6.2 Terrain analysis

### 6.2.1 Delineation of major morphological and hydrological characteristics

Analysis of slopes and relief (hillshaded DEM) reveal a complex landscape with both depositional (generally less than 1.5 degrees) and erosional landscape facets. The three main valleys in the areas including the Belalie, Bundaleer and Caltowie are separated by North-South orientated ridges and low hills. Local relief from the valley floors to the neighbouring ridges typically range from 500 to 750 metres. The Belaie, Bundaleer and Caltowie valleys have progressively lower base level elevations, suggesting regional tilting of basement rocks to the west. The valleys are formed by erosion of softer basement rocks whereas steep ridges are associated with resistant quartzite and siliceous tillites and siltstones. These valleys are partially filled with a series of coalescing alluvial and colluvial fans that receive sediments from the surrounding hills and ridges. The fans appear as a series of broad lobes radiating from the base of low hills and ridges, particularly within the Belaie and Bundaleers valleys. Gradients on these fans are low, with a range of 0.2 to 1 degrees (Figure 17).

Alluvial flats occur along parts of the main axial drainage lines. Floodplain sediments associated with river flats consist of silts, clays and minor gravel beds. The valleys (particularly the Belalie) show distinct profile asymmetry, with gentle slopes east of the main axial channel and short steep valley slopes on the western side (Figure 18a and b). The asymmetry is due to bedrock competency contrasts within the catchment and regional tilting as described previously. The eastern side of the catchment

has eroded into relatively soft metamorphosed sediments as apposed to the western side that is bounded against steep quartzite ridges. Most of the valley sediment comes from the east and as a consequence the main stream in the catchment has been confined to the western edge of the valley. The position of the stream is likely to have changed little as the valley was progressively filled with sediment. This conclusion is supported by the distribution of the magnetic channels that are concentrated along the western edge of the valley floor.

Pediments are also an important landform feature in the region. They form low relief erosional surfaces with a discontinuous and generally thin alluvial mantle over weathered bedrock. Pediments commonly occur as a transitional zone between rises and low hill, and alluvial sheet flood fans. Pediments are best developed over the upper parts of the Caltowie catchment (Figure 18b – profile 5).

Drainage patterns are weakly dendritic to sub-parallel with trellis patterns controlled by North-South trending structures. Streams are intermittent and flow mainly in the wetter winter months. In many cases the lower order tributaries are discontinuous (Figure 3) suggesting a significant amount of local groundwater enters the alluvial and colluvial sediments.

Drainage lines interpreted from the digital elevation model (Figure 19) indicate drainage that may develop if there is sufficient rainfall to cause surface saturation and runoff. The modelled network effectively connects the discontinuous drainage pattern shown on the topographic maps. These DEM derived drainage lines can be seen as a proxy of likely surface and near-surface water flow in the valley systems. Colour coding the channels according to their slope helps to highlighting zone of possible stagnation as well as areas with well drained surface flow systems (Figure 19). Steep slopes are associated with rises and hills with progressively lower slopes associated with pediments, alluvial fans and floodplains. Low gradient streams correlate with the modelled distribution of surface silt (Figure 15) and further supports the hypotheses that the silts were deposited in a low energy environment and possibly as a suspension load deposit.

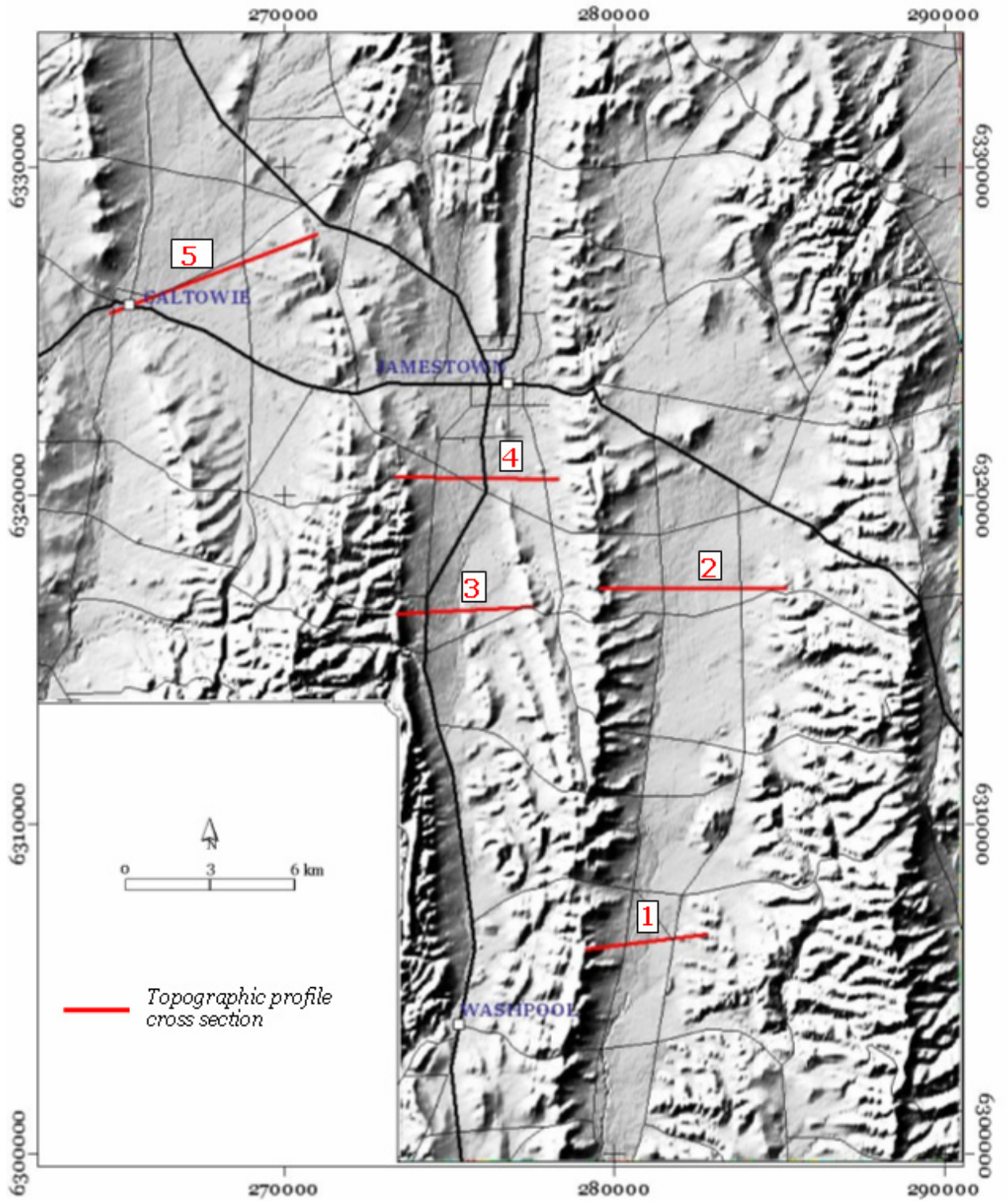


**Figure 18. A** - Location of topographic x-sections across the Belalie, Bundaleer and Caltowie valleys.

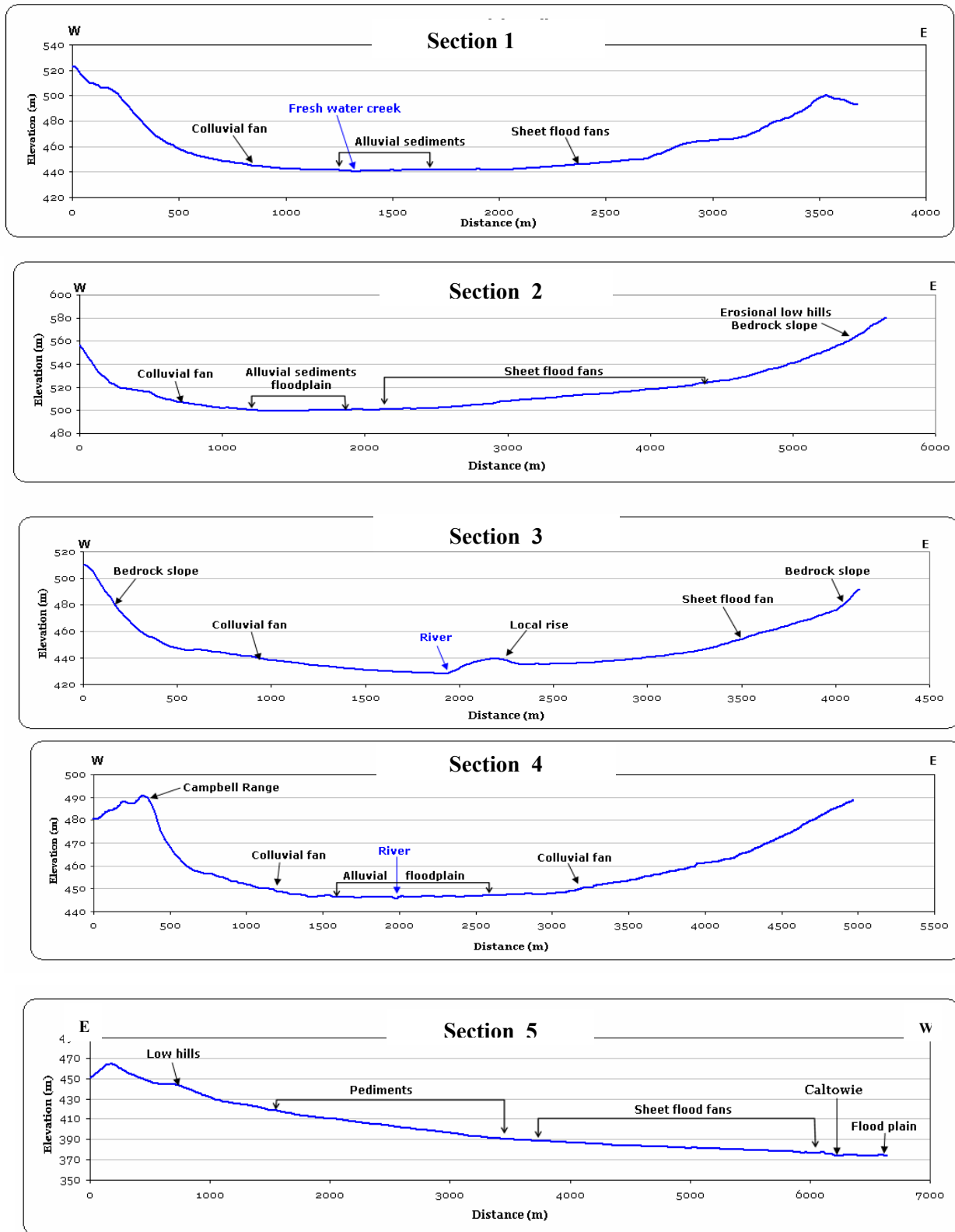


**Figure 18. B** - Topographic profiles across the Belalie, Bundaleer and Caltowie valleys. Refer to figure 18 A for locations.

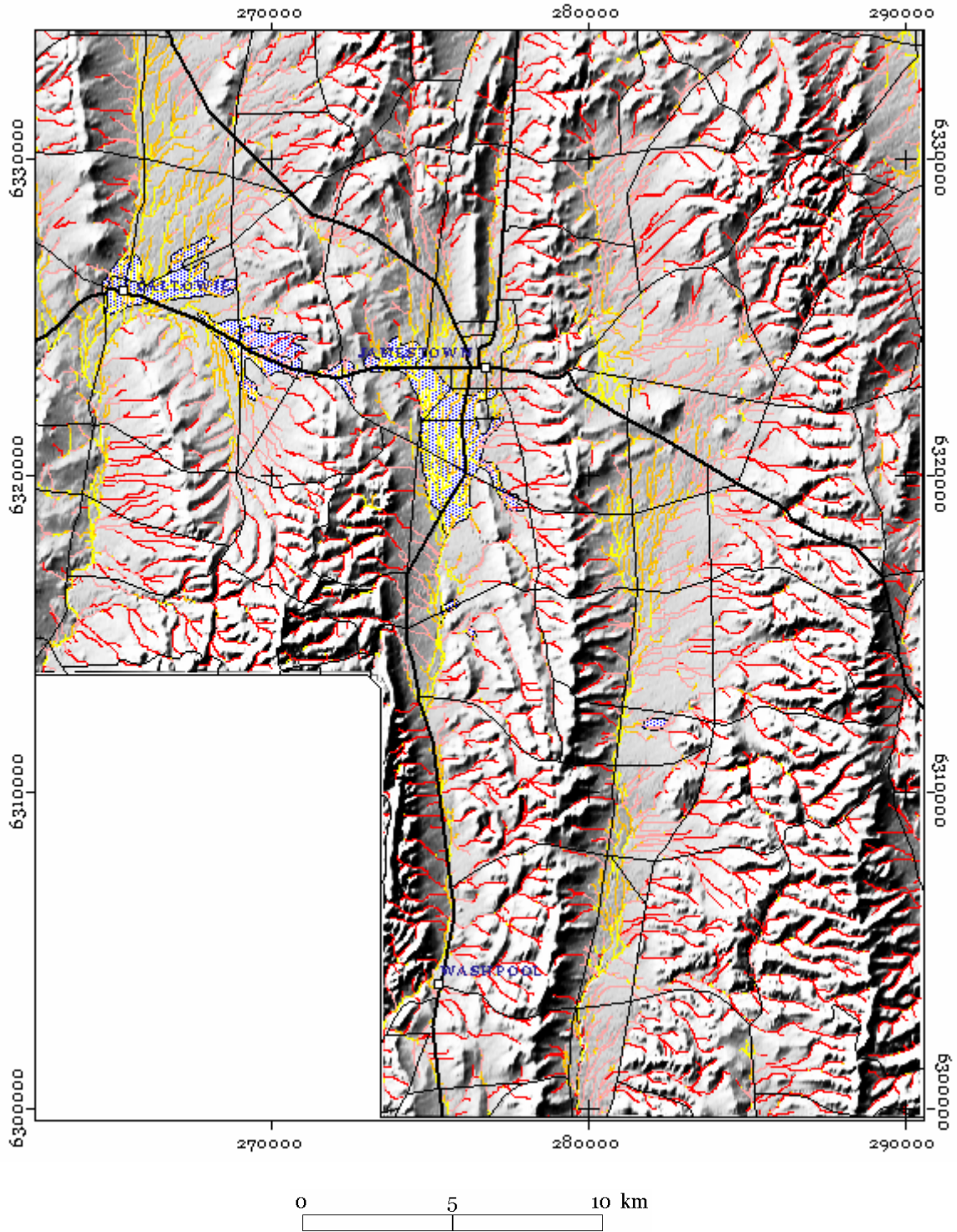


**Figure 19.** Drainages derived from the digital elevation model. Drainage segments are coloured according to their gradients. Low stream gradients in yellow – higher gradients in pink to red.

## 6.3 Interpretation of airborne magnetics

### 6.2.1 Delineation of magnetic drainage channels

Analysis of the airborne magnetics imagery provides insight into the palaeo-landscape. The most striking feature in the magnetic imagery is an intricate dendritic to sub-parallel drainage pattern superimposed over a larger scale north-south trending bedrock related magnetic response (Figure 20 and 21). These drainage features have a high frequency magnetic response and correlate with near surface (<1m) and buried (up to 40m) maghemite-bearing river channel gravels and sands. The maghemite materials consist mostly of ferruginised lithic granules and to a less extent larger lithic fragments and angular to sub rounded ferruginous gravels. These detrital clasts are likely to have eroded from weathered basement rocks, soils and lags on neighbouring hills and ridges. Various origins of the formation of maghemite have been put forward. Heating from bush fires and lightning strikes can also convert goethite to maghemite (Anand and Gilkes, 1987). Under suitable conditions biological processes can precipitate magnetic iron oxide crystals (Stolz, et al., 1986). Both processes may play a role in the Jamestown region. A proportion of the magnetic response might also relate to primary magnetic granules derived from the weathering of the bedrock. Determining the origin of the magnetic materials in the sediment deposits requires further investigation.

Superimposing present day drainage over magnetic palaeo-drainage lines provides clues about how the streams may have evolved through time and the shape of valleys prior to alluviation. Present day low order streams correlate spatially with the magnetic patterns. However, the filled channels in the axial part of the valley floor show considerably more complexity and density than the contemporary surface drainage (Figure 20 and 21). The position of low order magnetic stream channels is controlled by the local topography. These channels are 'fixed' by the local relief and tend to form narrow discrete magnetic channel patterns. Drainage patterns tend to be dendritic or rilled where they drain from steep ridge lines. Within the buried valley fill sequence the control of basement topography on stream position is reduced and the palaeo-channels shift position as the valleys were progressively filled with sediment. This is reflected in an inter-woven magnetic network stream channel pattern seen in the magnetic imagery. In places the magnetic image has a blurred or diffuse response. This may reflect the development of a braided river channel system with many small gravel or sand stringers, or stacking and shifting of discrete river channels as the valleys filled with sediment. Alternatively, blurring of the magnetic signature might be due to a thicker accumulation of non-magnetic clays and silts. In places, where streams have incised gullies into the valley alluvium the abundance of silt and clay in the exposed sections would suggest the latter is the most probable explanation.

There is clear evidence of superimposed drainage that has diverted palaeo-drainage lines east of Jamestown and created a new local drainage divide. Prior to alluviation of the Belalie valley, the magnetic drainage patterns indicated that all the streams flowed south (Figure 22a). However, the upper part of the stream that now passes through the township of Jamestown and into the Bundaleer valley, flows away from that indicated by the magnetic drainage directions (Figure 21b). This is likely to have been caused by sediments infilling the Belalie Valley to a point where the ridge separating the Belalie and Bundaleers valleys was breached. This occurs just north-east of Jamestown. Streams that evolved across this depositional surface flowed east/west over the now buried ridge that once separated the two valleys. The contemporary drainage has now incised a deep gorge into the sediments and basement ridge. As a consequence a new catchment divide has developed in the upper part the Belalie catchment. The upper tributaries of the Belalie valley have now been diverted into the Bundaleer catchment (Figure 22b), although sub-surface groundwater may still flow south into the Belalie valley catchment (Figure 22a). From a hydrogeological perspective, this has important implications for managing salinity in the area. Further study is needed to ascertain the significance of links between surface and deeper groundwater flow.

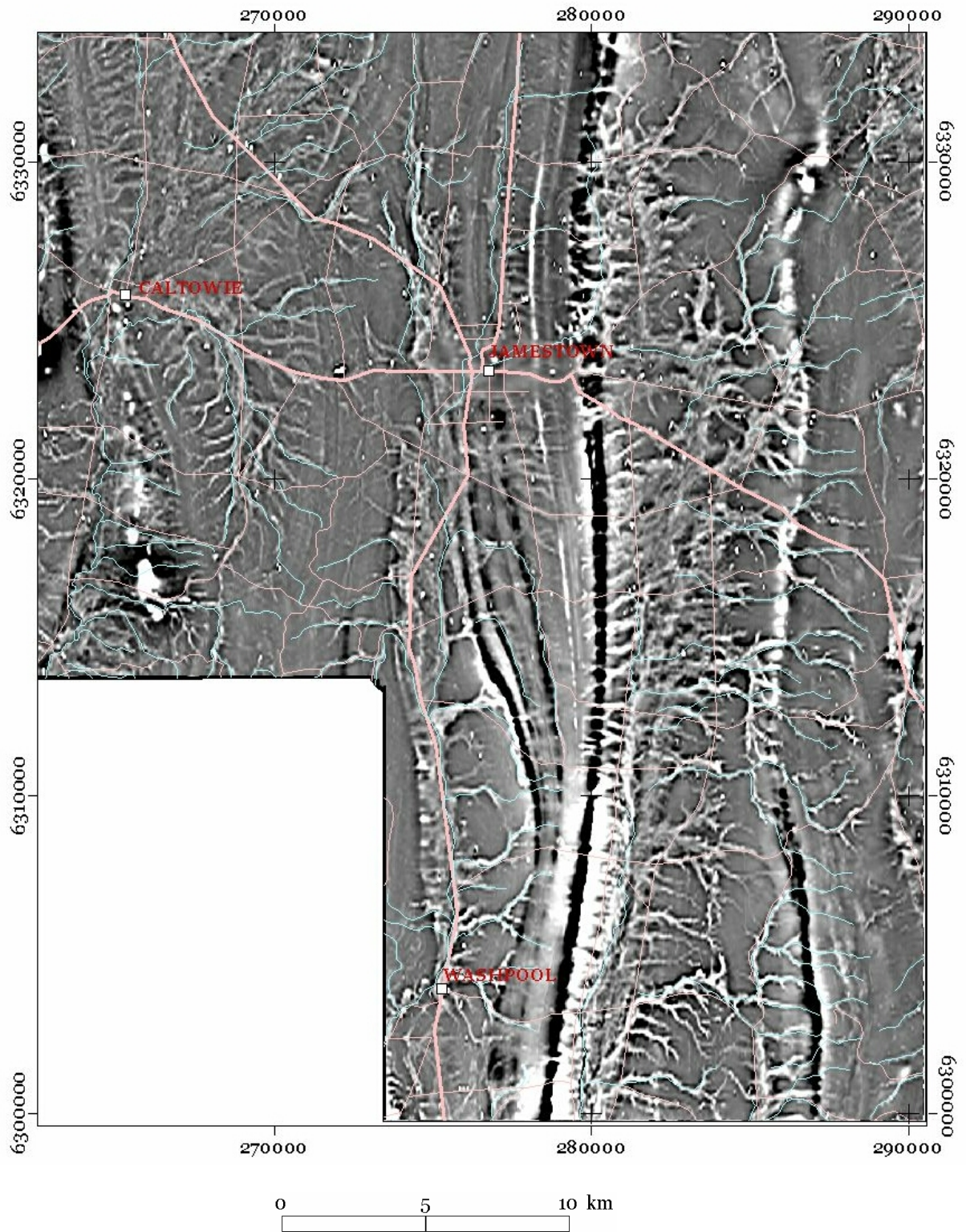


**Figure 20.** Magnetic image showing magnetic channel drainage lines and present day drainage in blue.

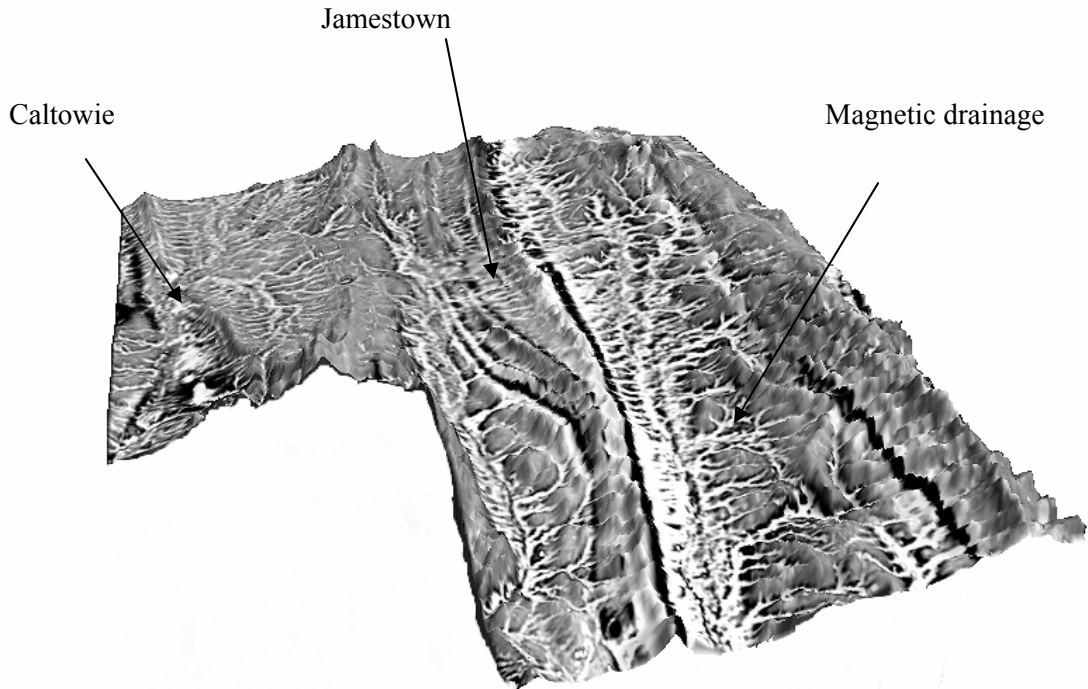


**Figure 21.** Perspective magnetic image highlighting magnetic river channels draped over the DEM.

A

B

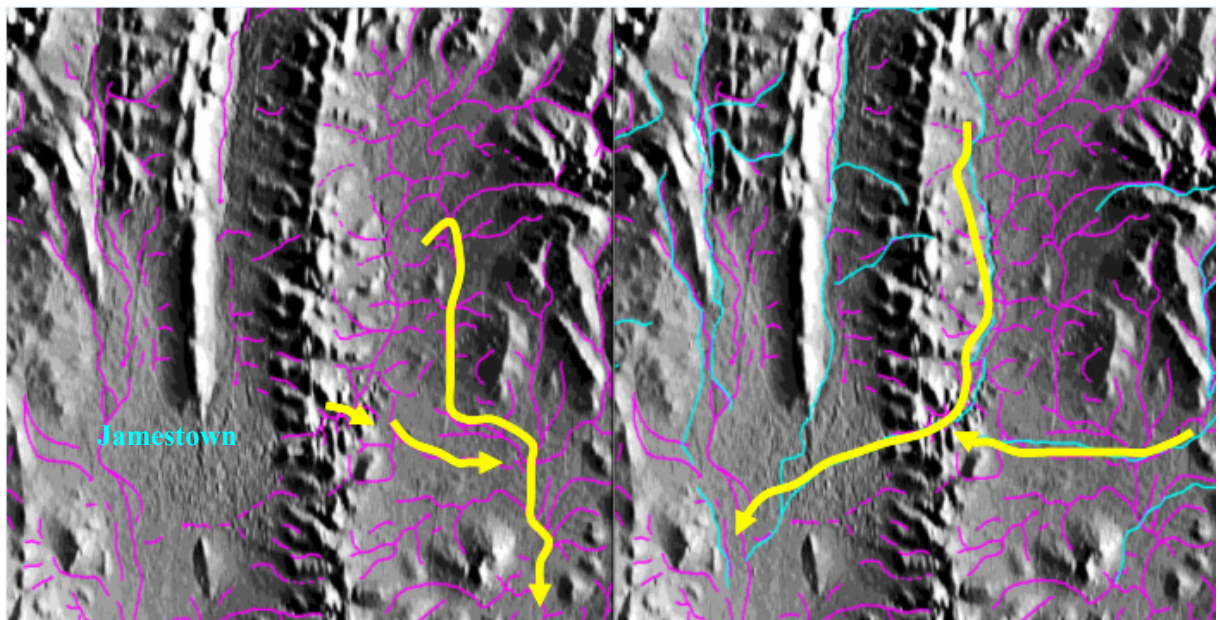


**Figure 22.** A – Original drainage network (purple) and flow direction (yellow) as delineated from the magnetic drainage lines. B – Superimposed drainage developed as a result of infilling the upper part of the Belalie valley. Surface drainage now flows into the Bundaleer valley, although sub-surface groundwater is likely to still flow down the Belalie Valley.

#### 6.4 Interpretation of airborne EM

Analysis of the AEM (CDI'S – interval conductivities) data showed that high near-surface conductivity, to a depth of approximately 30 m, correlates with the valley sediments. Areas of high conductivity probably relate to sediments (alluvial clays and silts) with higher porosities and moisture content compared with the underlying saprolite and saprock. The palaeo-drainage lines identified in the magnetics correlate with zones of high conductivity, particularly in the 0 – 20 m depth range (Figure 23). The valley fill sediments probably act as pathways for preferential ground water flow across the landscape, and as a consequence these materials are likely to accumulate salt and water.

The high observed conductive response is a result of these processes. Most of the bedrock appears resistive (blue in image – Figure 9) with the exception of several discrete lithological units (possibly pyritic shales). These conductive basement rocks can be clearly seen and separated from the more recent conductive surficial sediments in the deeper interval conductivity slices. (eg > 40m, figure 9). Colluvial fans along the eastern edge of the Bundaleer Ranges and south from Caltowie have moderate conductivities in the shallow 0 - 15 m depth range. High near-surface conductivities to a depth of 20 metres NNW of Caltowie (western edge of the survey area - figure 9) may relate to a combination of colluvial deposits and highly weathered basement rocks. Rocks in the area are highly weathered and mottled with distinct clay and iron segregations in the weathering profile (Figure 27D) (see section 6.5).

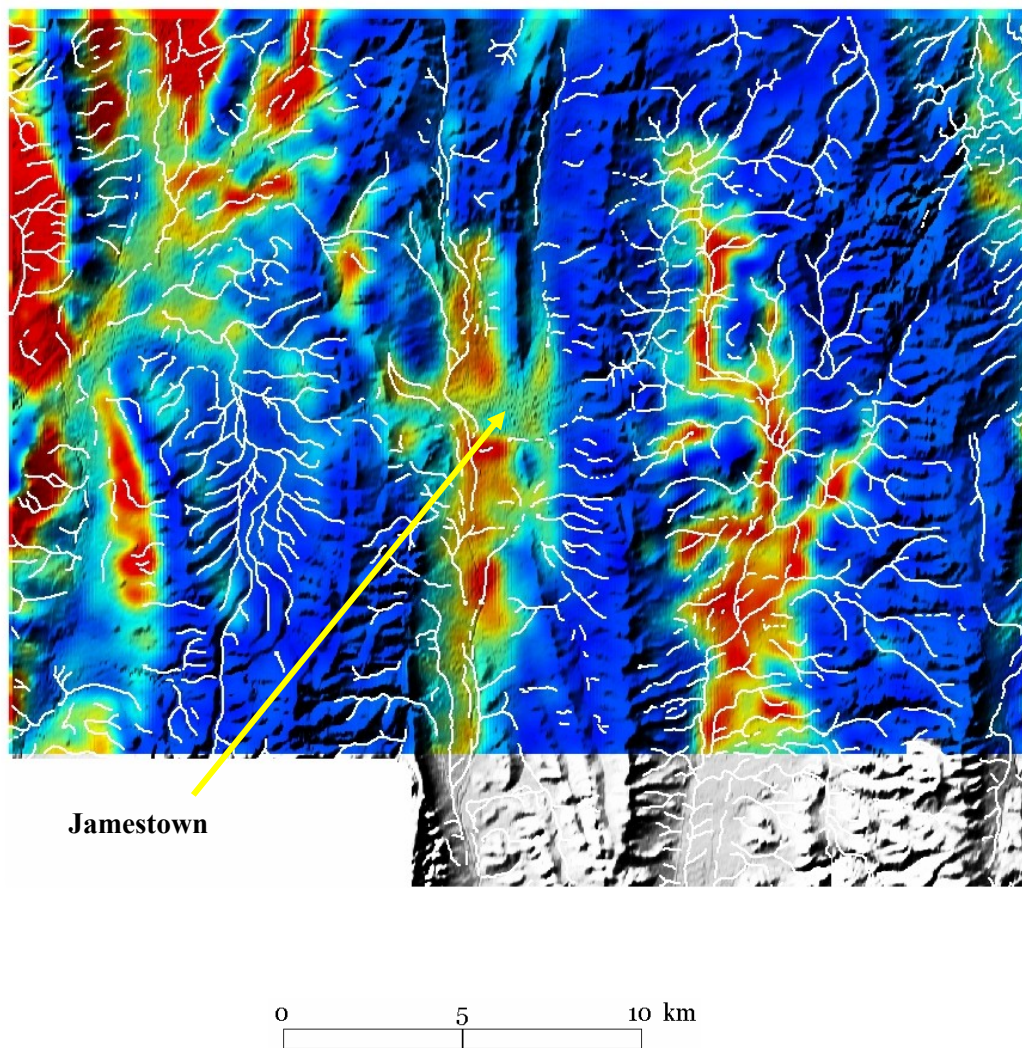


**Figure 23.** Magnetic drainage lines superimposed over the 10-15 m CDI slice.

The depth of transported sediments derived from drill hole interpretation correlates in most places with the transition between high and low conductance in the AEM data (e.g. the lower inflection point in the conductivity profile). It is difficult to resolve the sediment/saprolite contact, particularly where the basement rocks are highly conductive (i.e. pyritic shales) or where the saprolites are well developed. Drilling data suggests that the thickest sediments occur in the Belalie and Bundaleer valleys. In the Caltowie valley recent sediments are shallower with pediments dominating the upper parts of the catchment. The 15-20 interval conductivity highlights these differences (Figure 9) where the Caltowie catchment is considerably more resistive compared with the Belalie and Bundaleer catchments.

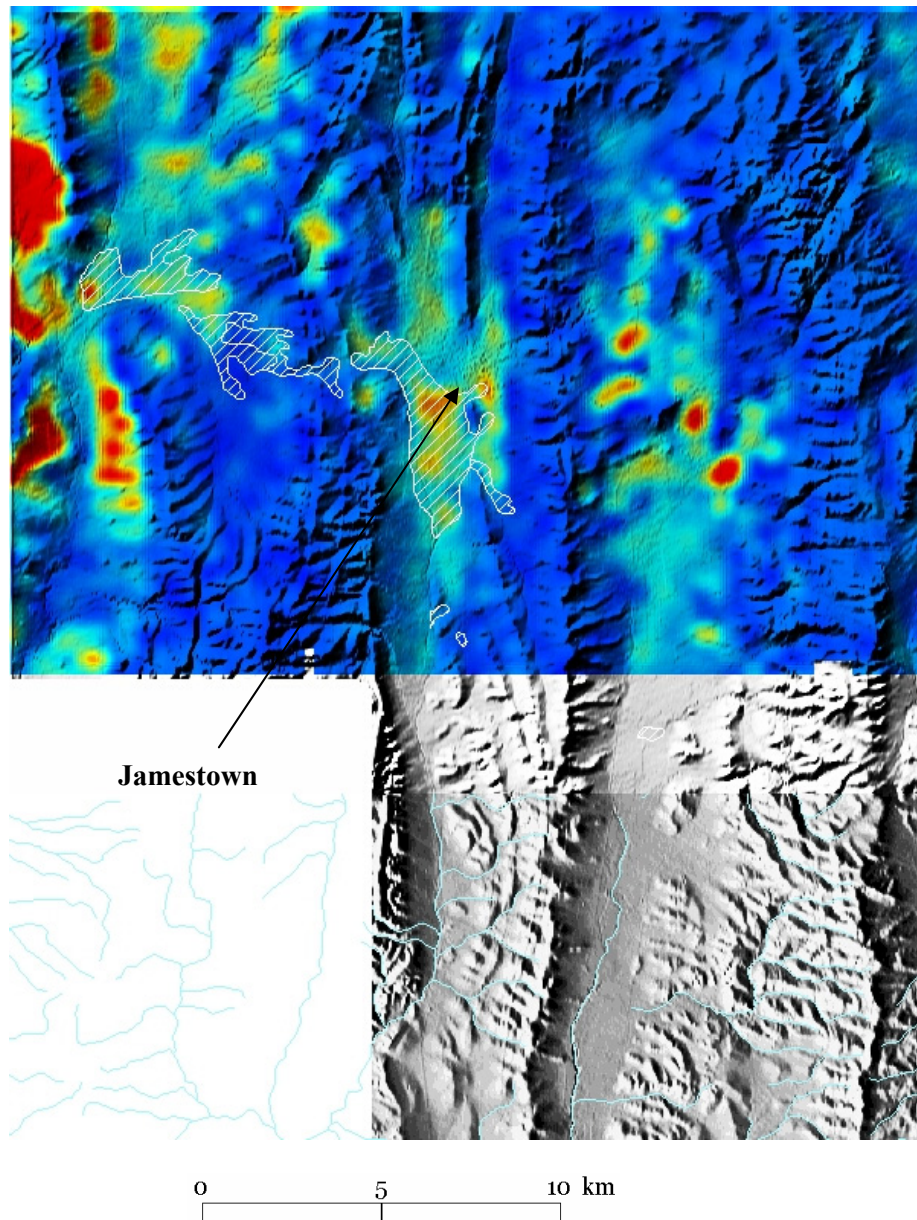


**Figure 24.** 0-5m CDI with areas of known dryland salinity (white polygons).

High conductivities in the 0-5m interval conductivity correlates with known areas of shallow water tables and land salinisation (Figure 24). Major areas of land affected by salt include alluvial sediments south of Jamestown in the Bundaleer valley and sediments near the township of Caltowie. In both cases the areas of salinised land occurs up stream from valley constrictions. It is proposed that these constrictions act as barriers to groundwater flow, promoting discharge. The high conductivities seen in the shallow interval conductivities may be related to fine grained sediments with high porosities (e.g. silt and clay) and near-surface saturation of these sediments with more saline groundwater.

## 6.5 Sedimentary Facies

Analysis of the sediments from gully exposures and drilling reveals three main forms of deposition: debris flow, traction and suspension load deposits. Debris or mudflow deposits are probably the most common type of sediment infilling the valleys. Debris flows have high viscosities and are poorly sorted with larger clasts floating in a much finer clay and silt matrix (Figure 26D). In places, cut and fill structures within these poorly sorted sediments suggest later reworking of debris flow deposits by channel erosion and deposition. Clasts are often orientated long axes parallel to the flow direction. The clasts include gravel size fragments of moderately and completely weathered saprolite, quartz, ferruginous saprolite and maghemite gravels and granules. Debris flow deposits are likely to be associated with sediments derived from coalescing alluvial and colluvial fans in filling the main north-south trending valleys.

Traction deposits are associated with stream channels where sediments are either transported by rolling, sliding or bouncing along the floor of the channel. They appear as discontinuous clast-supported gravel lenses in the sedimentary sequence. The clasts are typically imbricated and consist of gravel and coarse sand size saprolite fragments, ferruginous saprolite (some of which are magnetic) and quartz pebbles. (Figure 25F, 26E). The channels probably formed a braided network since most of the gravel deposits have a largely random vertical and lateral distribution. A braided stream network is also indicated by the irregular interwoven magnetic channel patterns seen in the airborne magnetics (Figure 20). In the Belalie and to a lesser extent the Bundaleer valleys sub-linear to weakly radial channels flow into the main axial drainage line from the valley sides (Figure 20).

In places fining upward sequences occur, that grade from clast supported gravels to fine sands and gravels supported by a matrix of silt and clay. This is likely to reflect a transition from a high discharge flow regime to one with lower discharge and energy. The silts and clays were probably deposited from suspension during the winnowing stages of a flood event. It is likely that low energy suspension load deposits of silt and clay became more important as stream gradients became shallower as the valleys were filled with sediment. The correlation of silt (based on the modelled K channel in the radiometrics) along the main axial sections of the valley floors with low stream gradients suggest that they probably accumulated as low energy suspension deposits associated with low angle sheet flood fans and flood plains.

The clay and fine silt fraction of the valley fill have probable been derived from the weathering of siltstones and mudstones with the catchments and from reworking of aeolian dust deposits that were probably deposited under dryer climatic condition than at the present day. Aeolian dust materials have been recognised as a major source of sediment in similar quaternary valley fill deposits in the Flinders Ranges of South Australia (Williams, M., *et al.* 2001).

In places partially truncated palaeosols with structured (columnar, prismatic) and sometimes mottled B-horizons are buried in the alluvial sequence. These palaeosols represent a hiatus in sedimentation and a period of weathering where soil forming processes have modified the structure of the sediments. This is likely to have occurred in inter-channel areas that were sub-aerially exposed.

Pedogenic and groundwater carbonates occur throughout the valley fill deposits. Carbonates occur in the soils and sediments as irregular nodules, platy sheets (Figure 25E), powdery deposits and as cast features associated with roots and worm burrows (Figure 25C, 26C). Fluctuating water tables and drying at the surface favours the precipitation of carbonate in the near surface. Groundwater carbonates form more massive, nodular to sheet like structures compared with pedogenic carbonates. They are associated with zones of preferential ground water flow and areas where ponding can occur. These zones include the unconformable contact between the sediments and the underlying saprolite and gravel beds and more impervious clay and silt units within the sedimentary pile (Figure 26F).



**Figure 25.** A – Belalie valley, B – colluvial fan down slope from the Bundaleer Range, C – carbonate root casts, D – poorly sorted debris flow deposits, E – alluvial sediments with platy carbonate layers and F – channel gravels (traction deposit).

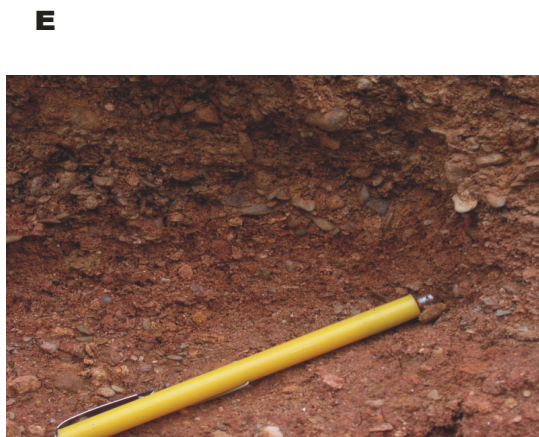


**Figure 26.** A – Carbonate precipitating along joints and fractures within the saprolite, B – eroded terraced alluvium eastern side of the Belalie valley, C – roots/worm burrows replaced by carbonate, D – highly weathered structured saprolite with a veneer of silty soil, E – maghemite gravels and F – groundwater carbonate precipitating along the saprolite – sediment contact.

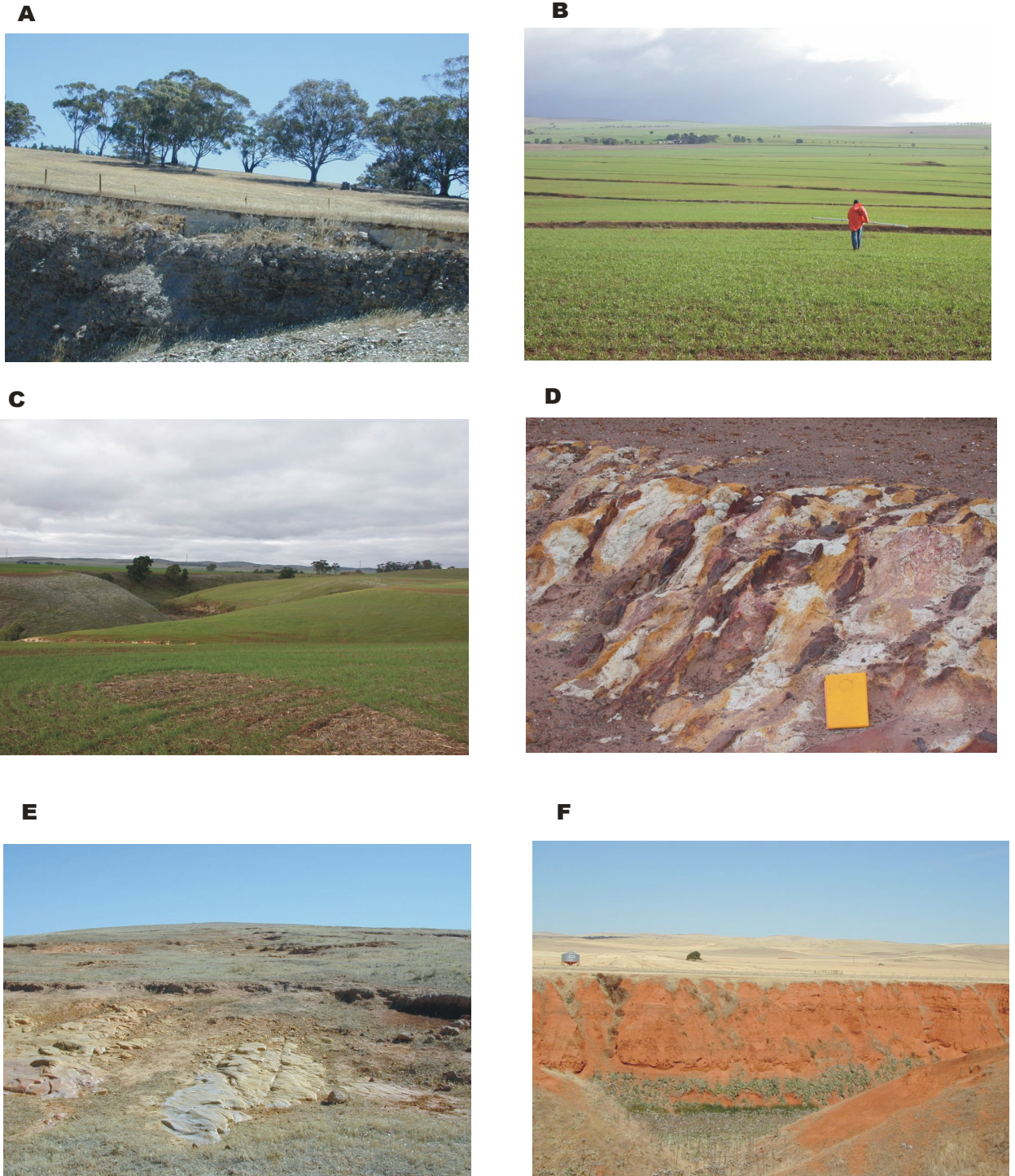


**Figure 27.** A – lithosols on bedrock, typically of the upland areas, B – low angle colluvial fan, C – incised sheet flood fan sediments east of Jamestown, D – highly weathered and mottled saprolite NNW of Caltowie, E – erosional scars on shallow soils on saprolite and F – valley fill sediments in the lower part of the Belalie valley. A significant proportion of the clays and fine silts in the valley sequence are probably aeolian dust derived.

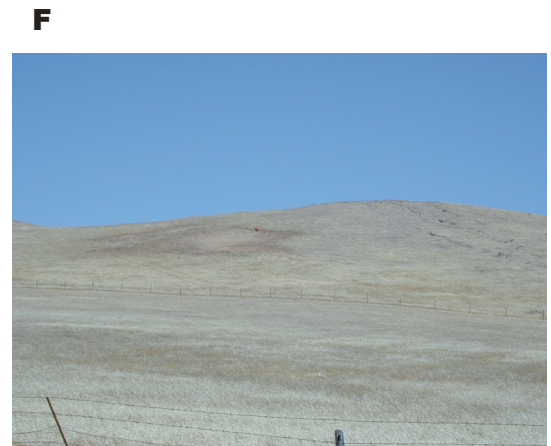


**Figure 28.** A – Rises in the upper part of the Caltowie catchment, B – river channel gravels consisting of ferruginous lithic fragments, quartz and minor maghemitic gravels, C – lithosols on low hills, D – dissolution depression caused by the removal of carbonate in the bedrock. These solution features collect water and are usually highly saline, E – incised alluvial sediments in the upper part of the Belalie valley and F – skeletal soils on low hills.

The contact between the sediment and saprolite may also be a preferential zone for the precipitation of silica and iron oxides. Ferricrete and silcrete were intersected in BRS holes JT2, 7 and 8 (Jones, et al., 2003) (Figure 31) at the base of the sediments. Silcrete at the base of the transported layer is thought to result from silica being mobilised in solution (Si source - quartzites and fine grained siliceous siltstones, sandstones) and then precipitated along the basal channel gravels and the porous higher weathered saprolite beneath the sediments. The ferricrete might have a similar origin since there is an abundant supply of iron in the basal ferruginous gravel layers.

### 6.6 3D architecture model of the evolution of the valley fill sequence and implications for salinity.

Analysis of the digital elevation model, gamma-ray spectrometry, magnetics, AEM and drilling provides insights into the 3D architecture (including geometry and composition) of the valley fill deposits (Figure 29). The thickest sediments (up to 40m) consisting of silt, clay, fine sand and minor gravels occur in the Belalie and Bundaleer valleys.

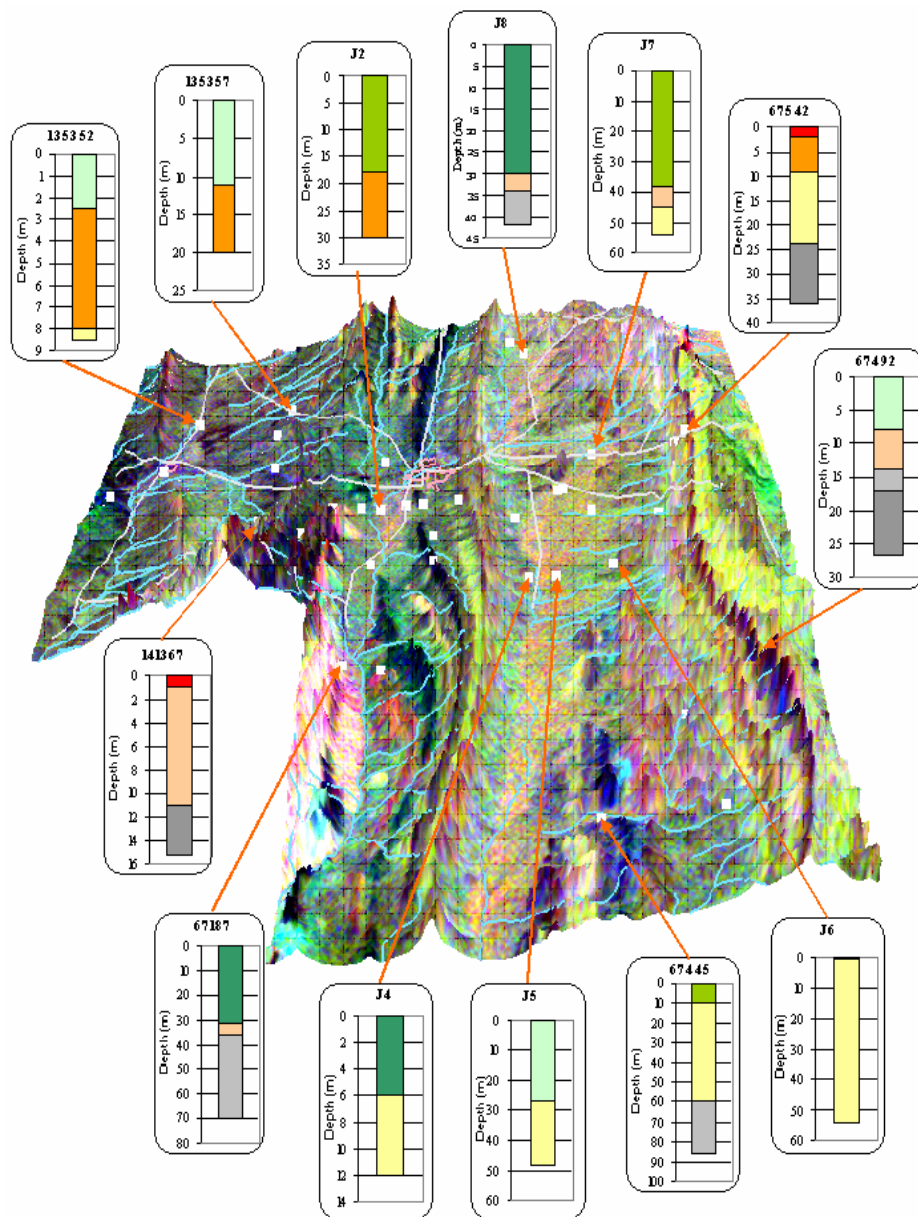


**Figure 29.** Position of selected drill logs and 3D perspective gamma-ray image (see figures 10 and 11).

The Caltowie valley has a thinner cover of sediment and is less conductive than the other two catchments. The valley fill sediments have not been dated but are likely to be Quaternary in age, although Tertiary sediments are associated with the Walloway Basin (Alley and Lindsay, 1995) north of Jamestown (approximately 25km).

Lignitic shales occur in the basal Tertiary sequence of the Walloway Basin (Figure 30) whereas no lignitic shales have been found in the Jamestown area or any indication of a major discontinuity in the sedimentary sequence to suggest older more weathered Tertiary materials. Surface soil texture analyses indicate that Caltowie valley has less silt and a higher percentage of medium and fine sand. Whether these sandy textures are a characteristic feature throughout the sedimentary sequence is not known. With the exception of some local discrete conductive basement rocks the sediments and some areas of highly weathered saprolite are the most conductive materials in the landscape.

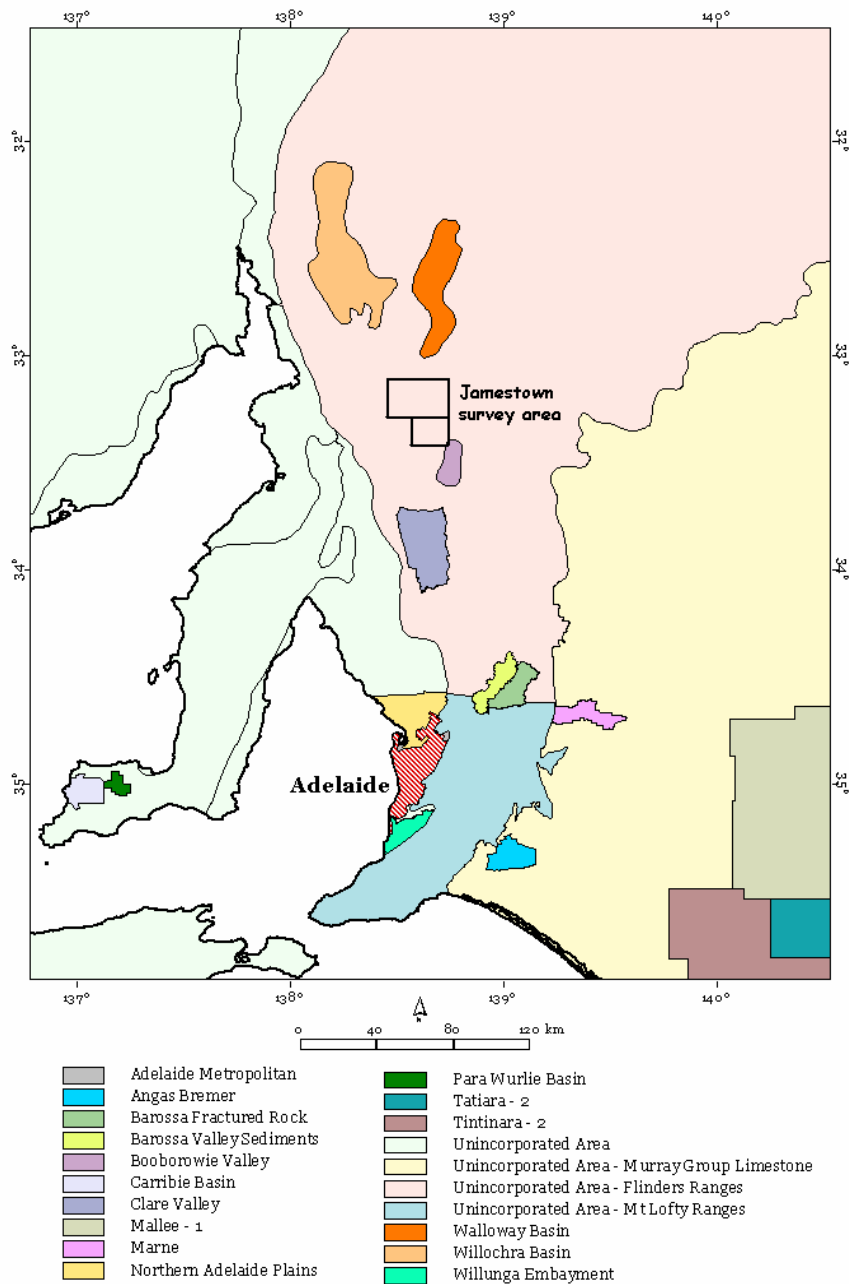


**Figure 30.** Major groundwater basins and agricultural districts (source: Department of land Water and Biodiversity Conservation).

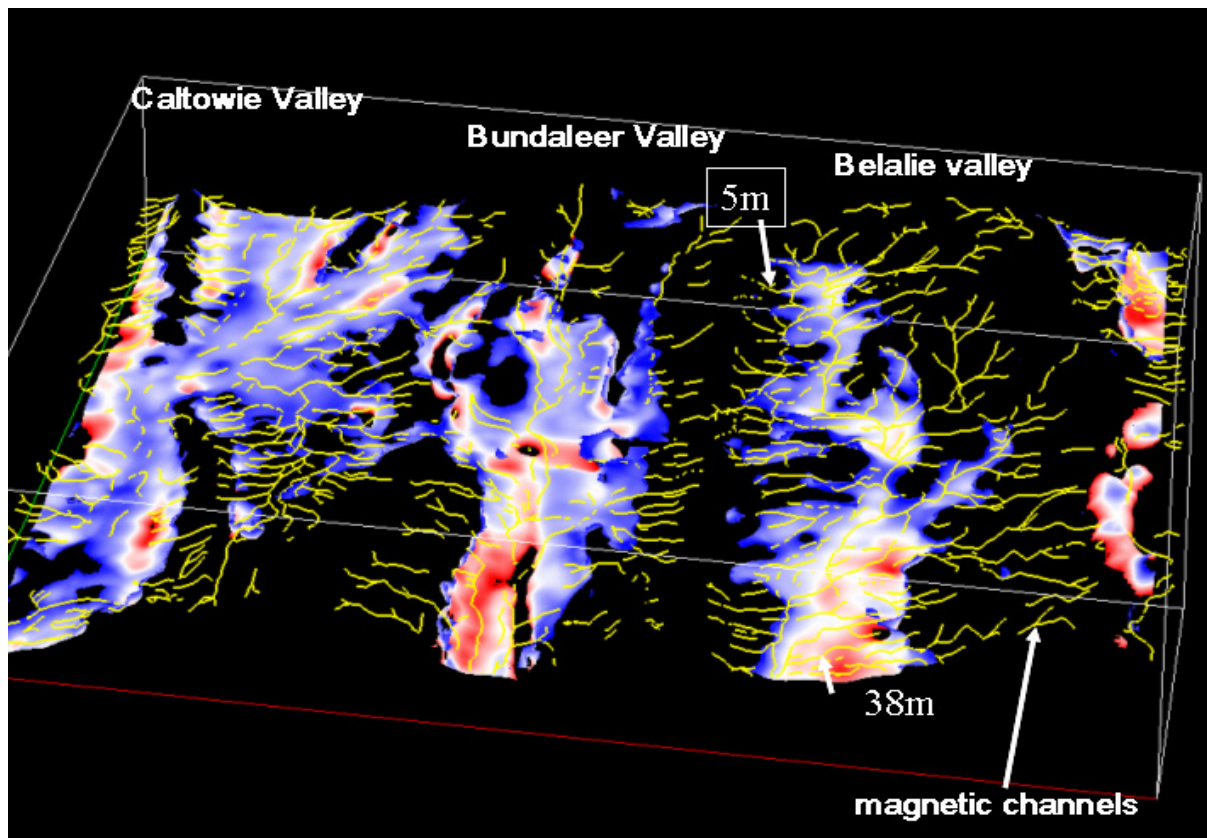


**Figure 31.** Base of the AEM conductor (50 m/Sm threshold used) coloured according to the thickness. In most cases this represents the sediment isopach in each of the three main valley systems. Indicative thickness of sediments shown. Magnetic channels in yellow. Conductive basement rocks are difficult to separate from the valley sediments. However they are generally much deeper features and can be easily identified in the imagery.

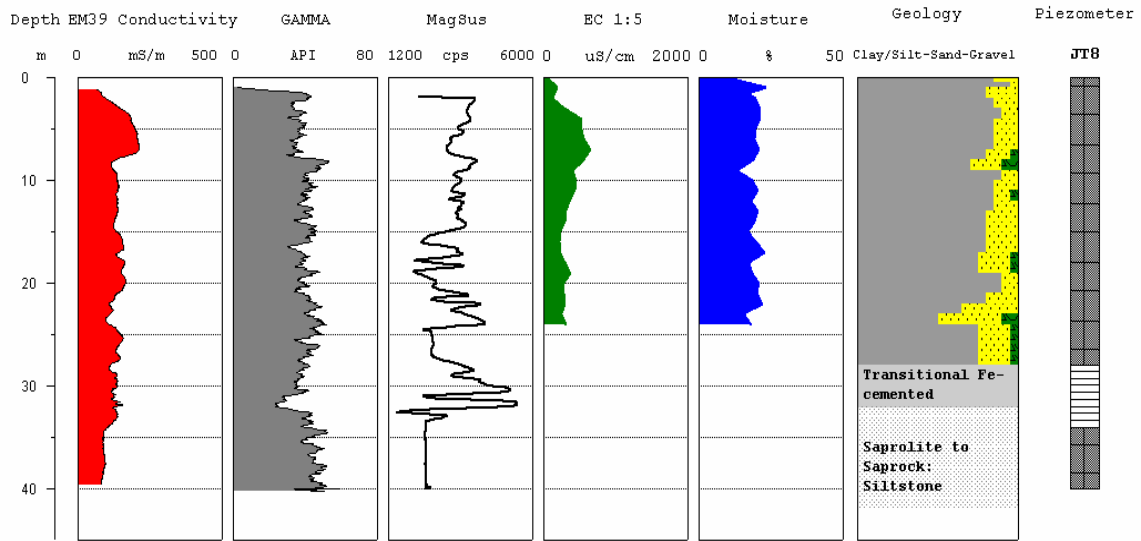
An isosurface (3D surface of equal value) of the high shallow conductance effectively delineates the geometry of the valley fill materials (Figure 31). Local scale textural variations within sediments (ie. channel gravels vs silt and clay) are not resolved by the AEM - but the main depositional patterns are clearly identified. In places, part of the high conductive response also incorporates very highly weathered (Figure 27D) and conductive bedrock materials (ie. pyritic shales) beneath the sediments. These conductive materials are not easily separated from overlying sediments in the AEM dataset. Both the fine grained sediments and the highly weathered bedrock are likely to contain the highest salt stores. This is supported by EC1:5 profiles (Jones and Henschke, 2003) that show conductivity bulges in the fine grained sediments and in the upper, generally more highly weathered saprolite materials (Figure 32). Weathering increases the capacity to store saline water because clays generated by the breakdown of primary rock minerals have generally much high porosity than the original bedrock.

From a sedimentological perspective the gravel deposits have a variable vertical and lateral distribution. The gravel layers range from poorly sorted matrix supported clasts through to moderately well sorted, clast supported fabrics. Drill logs indicated that the lower two thirds of the valley fill has a higher proportion of coarse grain sediments and more frequent gravel layers (e.g. Figure 32). The increase in the number of gravel deposits in the basal part of the sequence may



PROJECT: SA NAP - JAMESTOWN

HOLE\_ID: JT8 DATE: 11-12/04/2003 EASTING: 0280999 NORTHING: 6330687 EOH: 42 m

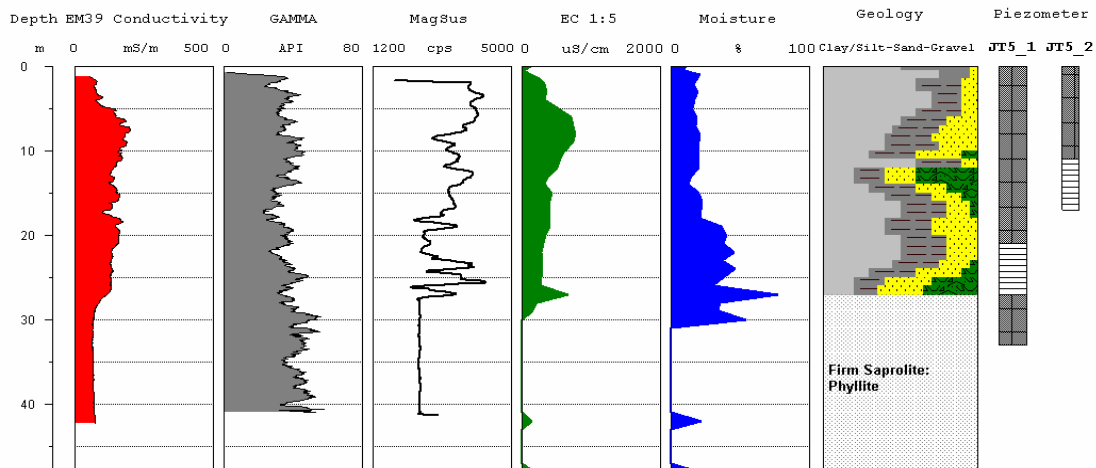


AGRICULTURE, FISHERIES AND FORESTRY - AUSTRALIA



PROJECT: SA NAP - JAMESTOWN

HOLE\_ID: JT5 DATE: 13/04/2003 EASTING: 0282187 NORTHING: 6315649 EOH: 48 m



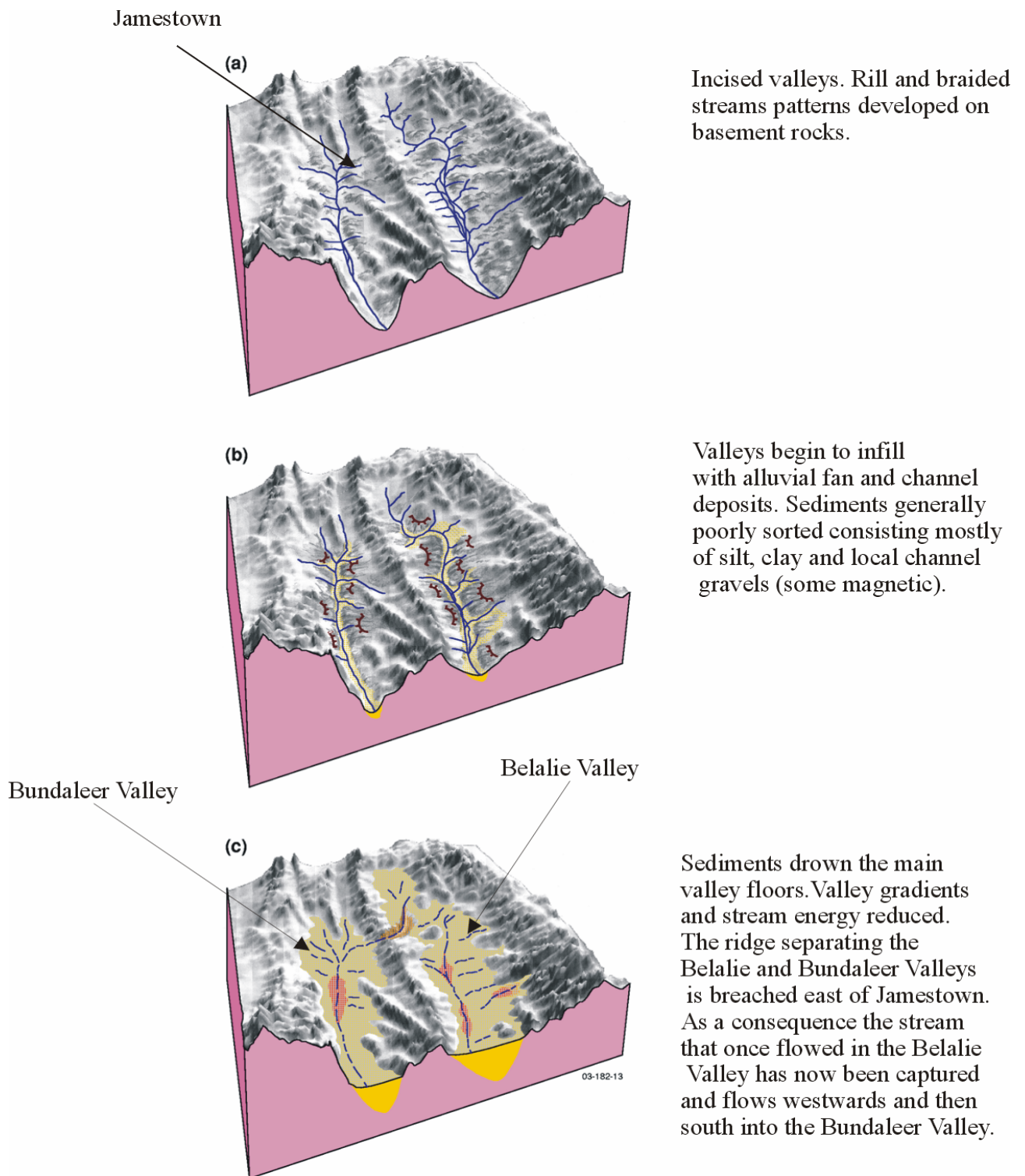
AGRICULTURE, FISHERIES AND FORESTRY - AUSTRALIA

Figure 32. BRS holes JT8 and JT5 showing geology, EC 1:5, moisture, gamma, EM39 and magnetic susceptibility. See figure 29 for location. JT8 occurs at the top of the Belalie valley; JT5 to the south in the thickest alluvial sequence.

reflect streams with relatively steeper gradients and higher energies. As the valleys filled stream gradients would have been lowered favouring the deposition of finer textured sediments. Alternatively, the changes in deposition might be in response to changes in climate (i.e. rainfall, runoff). From a hydrogeological perspective, the basal sedimentary layer, where channel gravels are more common and probably better inter-connected, is likely to have the highest hydraulic conductivity and potentially the greatest transmissivity. The unconformable contact between the sediments and the saprolite also appears to be a major zone of higher hydraulic conductivity. Carbonate, iron and silica have precipitated along the saprolite – sediment contact. The precipitation of these cements and the likely low transmissivity of the saprolite would promote lateral groundwater flow along the sediment – saprolite interface.

Overlaying areas of high conductivity (that in most cases relates to highly weathered saprolite and fine grained sediments) with palaeo-channels inferred from the magnetics, highlights potential salt stores and the likely conduits through which groundwater might flow. Further work on the channel gravels is required to determine their connectivity and transmissivity properties. Salinisation in the Jamestown region appears to correlate with areas identified in the AEM data as being more conductive. There may also be a causal link with the thinning of sedimentary cover where basement barriers or constrictions occur. This is observed in the Bundaleer and Caltowie valleys but not the Belalie valley despite the fact that the Belalie valley has a thicker sediment fill and potentially a higher salt store. One explanation might be that the Belalie system with its thicker sedimentary fill has a more interconnected buried channel network system. This more effective sub-surface drainage may therefore prevent the build up of shallow water tables and associated salts in the upper regolith or soil layer.

Interpretation and integration of drill hole logs, AEM, magnetics and gamma-ray spectrometry has been used to reconstruct the landscape from the early Quaternary to the present day for the Belalie and Bundaleer catchments (Figure 33). The model shows the evolution of stream drainage and sedimentation as the valleys became progressively choked with sediment.



**Figure 33.** Regolith-landscape evolution model for the upper part of the Belalie and Bundaleer River catchments. Landscape model based on drilling, terrain analysis and geophysical interpretation. A significant proportion of the sediment in the valleys is probably derived by aeolian dust that has been deposited and later reworked by hill slope processes and incorporated in the valley fill deposits.

## 7. CONCLUSIONS

A combined interpretation of gamma-ray, magnetics, digital elevation and AEM with information from drill holes was used to build a 3D architectural model of the valley fill sequence. New insights on how the landscape has evolved through time resulted. Also an improved understanding of the links between regolith, landforms and dryland salinity were developed. 3D models generated from the analysis and integration of these datasets shows the distribution of regolith materials, salt stores and likely conduits and, barriers to groundwater flow.

Gamma-ray imagery provides information on the geochemical variations of soil/regolith and bedrock materials. Gamma-ray spectrometry can highlight specific soil attributes when interpretations are made within major geological and geomorphic domains (e.g. erosional vs depositional). The distribution of surface silt content was determined in depositional landscapes using airborne K concentrations. The relationship between soil texture and K, related to silt size illite and K-mica in the soil. The magnetics provide excellent delineation of buried channel gravels. The older drainage mapped by the magnetics was a moderately closely-spaced dendritic to braided network. This contrasts the contemporary drainage that is widely spaced and discontinuous. The AEM dataset delineates areas of conductive basement and valley deposits consisting largely of silt and clay. Low conductive responses are associated with moderately weathered to unweathered metasediments. With the exception of some local conductive bedrock units (i.e. pyritic shales) the base and isopach of the sediments within the major valleys is determined by modelling the AEM data due to the contrast between the conductive sediments and underlying resistive basement rocks.

The major salt stores defined from drilling are associated with the valley fill materials which have been drilled to a depth of 40m. These sediments are dominated by poorly sorted debris or mudflow deposits and to a lesser extent traction or channel bed load deposits. The bed load deposits are likely to have high transmissivities compared with the clay and silt dominated debris deposits. Highly weathered bedrock also has the potential to store salts due to their relatively high porosities, and low transmissivities. Highly weathered bedrock occurs beneath some colluvial fans, particularly NNW of Caltowie. Even though the Belalie Valley has a high inferred (based on drilling and AEM) salt store it has little surface expressed salinity. This is possibly due to a series of the well connected, buried channel gravel system (inferred from the magnetics) that provides good sub-surface drainage. This occurs in the Belalie valley. The contact between the sediments and the saprolite appears to be a major zone for groundwater flow. In several places carbonate, iron and silica have cemented basal alluvial gravels. The main expression of salinity appears to be associated with valley constrictions that impede groundwater flow and cause shallowing of water tables. This occurs in the Bundaleer and Caltowie Valley. In the Bundaleer valley the restriction is associated with narrowing of the valley and deposition of colluvial fan sediments down slope from the Bundaleer Ranges. The constriction in the Caltowie catchment is largely associated with bedrock ridges south and north of the Caltowie Township.

Previous studies in the area have identified three major expressions of surface salinity including dryland salinity associated with low lying areas due to rising groundwater tables, sub-soil transient salinity and salt scalds or “magnesia” patches on hill slopes. However, field observations suggest that the latter is likely to be an erosional feature caused by overgrazing followed by a high rainfall event(s) after a prolonged dry period. Salts associated with these erosional scars may relate to wetting and drying of the upper part of the saprolite. Another form of surface expressed salinity not describe in the literature but probably well known by the local farmers in the region is identified. This is where dissolution of carbonate from the bedrock has led to the development of solution pits or shallow depressions in the landscape. These subtle depressions vary in size from about 20 m to 100 m across. Salts accumulate in these depressions due to evaporation of ponded water (e.g. internal drainage). The solution pits are not very extensive but at local scales should be considered when developing on farm management plans.

## **8. ACKNOWLEDGEMENTS**

I wish to thank Richard Cresswell, Craig Liddicoat, Mark Thomas and Chris Henschke for support in the field and in providing datasets as well as an opportunity to exchange views and debate issues. I also wish to thank Tim Munday, Mike Craig, Richard Cresswell and Mark Thomas who reviewed and improved the report. Special thanks to Heike Apps and Joe Mifsud for the production of GIS maps and figures. Thanks to Andrew Fitzpatrick for reprocessing the AEM slices.

This study was made possible through funding support by the SA and Commonwealth Governments through the National Action Plan for Salinity and Water Quality, and CRC LEME.

John Wilford publishes with the permission of the CEOs of Geoscience Australia and CRC LEME.

## 9. REFERENCES

- Alley and Lindsay, 1995. Walloway Basin, In *The geology of South Australia, Volume 2, The Phanerozoic* (ed. Drexel, J.F and Preiss, W.V), Bulletin 54, Geological Survey of South Australia.
- Anand R.R., Gilkes R.J 1987. The association of maghemite and corundum in Darling Range Laterites, Western Australia. *Aust. J. Soil Res*;35:303-311
- Bulter B.E., 1982., The Location of Aeolian dust mantles in southeastern Australia, In: Wasson R.J. ed *Quaternary Dust Mantles of China, New Zealand and Australia*, 141-144. Australian National University, Canberra.
- Chartres, C. J., Chivas, A.R and Walker., P.H. 1988. The effect of Aeolian accessions on soil development on granitic rocks in southeastern Australia., *Oxygen-isotope, mineralogical and geochemical evidence for Aeolian deposition*, *Australia Journal of Soil Research* 26, 17-31.
- Chor, C., Nitschke, N. and Williams, M. (2003). Ice, wind and water: Late Quaternary valley-fills and aeolian dust deposits in arid South Australia. *Proceedings of the Cooperative Research Centre for Landscape, Environment and Mineral Exploration (CRC LEME) Regional Symposia, Advances in Regolith*, edited by I.C.Roach, Adelaide, November 13-14, 2003.
- Cooper, L., 1978. *Jamestown – A photographic Study*. Corporation of Jamestown.
- Cresswell, R.G. and Herczeg, A.L. 2004. Groundwater flow systems and salinity in the valleys around Jamestown, South Australia: Geochemical and isotopic constraints. CSIRO Land and Water Technical Report No. 30/04 / BRS Technical Report, June 2004
- Fitzpatrick, A., 2003, Calculation of conductivity depth images (CDI) SA AEM data using Emflow 5.30: TEMPEST: Riverland and Tintinara (East and West), RESOLVE: Jamestown and Angas Bremer Plains., South Australia Salinity Mapping and Management Support Project, CRCLEME Open file report 17
- Fugro Acquisition and Processing technical report, 2002a, Jamestown and Angas-Bremer Airborne Surveys. Airborne magnetic, gamma-ray and elevation surveys, (Prepared by S. Murphy and L. Stenning). Bureau of Rural Sciences. FAS JOB # 1545.
- Fugro Acquisition and Processing technical report, 2002b, Jamestown and Angas-Bremer Plains Airborne Surveys. TEMPEST Geophysical Surveys, (Prepared by M Owens and L. Stenning). Bureau of Rural Sciences. FAS JOB # 1544.
- Henschke, C. J., McCarthy, D.G., Richardson, S.B., and Evans, T.D., 1994. Investigation and management of dryland salinity in a catchment at Jamestown in the Mid North of South Australia, Technical Paper No 35, Primary Industries South Australia, ISBN 0 7308 4328 9.
- Henschke, C.J., Jones, G.L. and Cresswell, R.G. 2004. Groundwater investigations on valley fills, Jamestown, South Australia, BRS Technical Report, September 2004.
- Jones, G and Henschke, C., 2003, SA Salinity Mapping and Management Support Project: Jamestown drilling report, in prep.
- Lane, R. Leeming. P. Owens, M and Triggs, D. 1999. Undercover assignment for Tempest, Preview, no 82, October 1999, pp 17-21.

Macnae, J.C., King, A., Stolz, N., Osmakoff, A., Blaha, A., 1998, Fast AEM data processing and inversion: *Expl. Geophys.*, **29**, 163-169.

Minty, B.R.S., 1997 – The fundamentals of airborne gamma-ray spectrometry. *AGSO Journal of Australian Geology and Geophysics*, 17(2).

PIRSA Land Information 2001. *Soils of South Australia's Agricultural Lands*, (CD ROM). Primary Industries and Resources South Australia.

Rengasamy, P., 2002, Transient salinity and sub-soil constraints to dryland farming in Australian sodic soils: an overview, *Australian journal of Experimental Agriculture*, Vol43, no 8.

Stephens, C.G., Herriot, R. I., Downes, R.G., Langford-Smith., 1945. A soil, land-use; and erosion survey of part of Country Victoria, South Australia, Council for Scientific and Industrial research, Bulletin No 188.

Stolz, J. F., S.-B. R. Chang, et al. (1986). Magnetotactic bacteria and single-domain magnetite in hemipelagic sediments. *Nature* 321: 849-851.

Wilford, J. 1999. Scientific visualisation and 3D modelling applications for mineral exploration and environmental management, *AGSO Research Newsletter*, No 31.

Williams, M., Prescott, J.R., Adamson, D., Cock B., Walker K and Gell P., 2001. The enigma of a late Pleistocene wetland in the Flinders Ranges, South Australia. *Quaternary International* 83-85, 129-144.